Molecular Pharmacology Fast Forward. Published on August 27, 2015 as DOI: 10.1124/mol.115.099960
This article has not been copyedited and formatted. The final version may differ from this version.

Selectivity In The Use of $G_{i/o}$ Proteins Is Determined by the DRF Motif In CXCR6 And Is Cell-type Specific

Satya P. Singh, John F. Foley, Hongwei H. Zhang, Darrell E. Hurt, Jennifer L. Richards, Craig S. Smith, Fang Liao and Joshua M. Farber

Laboratory of Molecular Immunology (S.P.S., J.F.F., H.H.Z., J.L.R., C.S.S., F.L., and J.M.F.) and Bioinformatics and Scientific IT Program, Office of Technology Information Systems (D.E.H.), National Institute of Allergy and Infectious Diseases, National Institutes of Health, Bethesda MD 20892; and Howard Hughes Medical Institute-National Institutes of Health Research Scholars Program, Bethesda MD 20814 (C.S.S.).

Molecular Pharmacology Fast Forward. Published on August 27, 2015 as DOI: 10.1124/mol.115.099960
This article has not been copyedited and formatted. The final version may differ from this version.

Running title: Roles for non-canonical sequences in CXCR6

Address correspondence and reprint requests to Dr. Joshua M. Farber, Laboratory of Molecular Immunology, NIAID, NIH, Bldg. 10, Rm. 11N112, MSC 1886, Bethesda, MD 20892, USA. E-mail address: jfarber@niaid.nih.gov

Number of text pages: 48

Number of tables: 1

Number of figures: 8

Number of supplemental figures: 13

Number of references: 72

Number of words in Abstract: 244

Number of words in Introduction: 867

Number of words in Discussion: 1885

Nonstandard abbreviations: GPCR, G-protein coupled receptor; H3C, cytoplasmic end of the third transmembrane helix; FBS, fetal bovine serum; PCR, polymerase chain reaction; YFP, yellow-green fluorescent protein; MFI, mean fluorescent intensity; K_d, equilibrium dissociation constant.

Molecular Pharmacology Fast Forward. Published on August 27, 2015 as DOI: 10.1124/mol.115.099960
This article has not been copyedited and formatted. The final version may differ from this version.

Abstract

CXCR6, the receptor for CXCL16, is expressed on multiple cell types and can be a co-receptor for HIV-1. Except for CXCR6, all human chemokine receptors contain the $D^{3.49}R^{3.50}Y^{3.51}$ sequence, and all but two contain $A^{3.53}$, at the cytoplasmic terminus of the third transmembrane helix (H3C), a region within class A G-protein-coupled-receptors that contacts G proteins. In CXCR6, H3C contains $D^{3.49}R^{3.50}F^{3.51}I^{3.52}V^{3.53}$ at positions 126-130. We investigated the importance and inter-dependence of the canonical D126 and the non-canonical F128 and V130 in CXCR6 by mutating D126 to Y, F128 to Y, and V130 to A, singly and in combination. For comparison, we mutated the analogous positions, D142, Y144, and A146 to Y, F, and V, respectively, in CCR6, a related receptor containing the canonical sequences. Mutants were analyzed in both HEK-293T and Jurkat E6-1 cells. Our data show that for CXCR6 and/or CCR6, mutations in H3C can affect both receptor signaling and chemokine binding; non-canonical H3C sequences are functionally linked, with dual changes mitigating effects of single mutations; mutations in H3C that compromise receptor activity show selective defects in the use of individual $G_{i/o}$ proteins; and the effects of mutations in H3C on receptor function and selectivity in $G_{i/o}$ protein use can be cell-type specific. Our findings indicate that the ability of CXCR6 to make promiscuous use of the available $G_{i/o}$ proteins is exquisitely dependent on sequences within the H3C, and suggest that the native sequence allows for preservation of this function across different cellular environments.

Molecular Pharmacology Fast Forward. Published on August 27, 2015 as DOI: 10.1124/mol.115.099960
This article has not been copyedited and formatted. The final version may differ from this version.

Introduction

CXCR6 (known previously as STRL33/BONZO/TYMSTR (Deng et al., 1997; Liao et al., 1997; Loetscher et al., 1997)) is the seven transmembrane domain G-protein-coupled receptor (GPCR) for CXCL16, a chemokine that exists in both membrane-anchored and soluble forms (Matloubian et al., 2000; Wilbanks et al., 2001). CXCR6 is expressed on many cell types in the immune system (reviewed in (Bachelerie et al., 2013). CXCR6-expressing T cells are enriched at sites of inflammation in autoimmune disease (Kim et al., 2001), and CXCR6 on innate lymphoid cells is important for positioning of these cells in the gut during infection (Satoh-Takayama et al., 2014). CXCR6 can function as a co-receptor for multiple strains of HIV-1, as well as SIV (Alkhatib et al., 1997; Deng et al., 1997; Liao et al., 1997; Zhang et al., 2001). Although a role for this receptor in HIV-1 disease has not been established, recent data demonstrate an association between a polymorphism in *CXCR6* and long-term non-progression in HIV-infected individuals (Limou et al., 2010).

As compared with sequences for other chemokine receptors, the CXCR6 sequence contains a number of unusual features, including an absence of Cys residues in the N-terminal domain and the third extracellular loop, and a $D^{3.49}R^{3.50}F^{3.51}I^{3.52}V^{3.53}$ sequence at the cytoplasmic end of the third transmembrane helix (H3C). The canonical sequence for human chemokine receptors at this position is $D^{3.49}R^{3.50}Y^{3.51}X^{3.52}A^{3.53}$. Residue designations 3.49-3.53 are according to the convention of Ballesteros and Weinstein, in which positions are numbered in each helix with reference to the residue in that helix that is most highly conserved within class A GPCRs (Ballesteros and Weinstein, 1995). The high degree of conservation of the $E/D^{3.49}R^{3.50}Y^{3.51}$ motif in H3C has led to a series of investigations of the roles of these residues in receptor function. It has been proposed that in the inactive conformation, $R^{3.50}$ sits in an "arginine cage", in which $R^{3.50}$ interacts with $E/D^{3.49}$ (Ballesteros et al., 1998) and forms part of an "ionic lock", in which $R^{3.50}$ interacts with $E^{6.30}$ and from which it is liberated during activation (Ballesteros et al., 2001; Scheerer et al., 2008). As determined in crystal structures, in active conformations of opsin/rhodopsin, $R^{3.50}$ loses its interaction with $E/D^{3.49}$ and forms hydrogen bonds with $Y^{5.58}$ and a

Molecular Pharmacology Fast Forward. Published on August 27, 2015 as DOI: 10.1124/mol.115.099960
This article has not been copyedited and formatted. The final version may differ from this version.

backbone carbonyl group of the transducin α-subunit (Choe et al., 2011; Scheerer et al., 2008; Standfuss et al., 2011), whereas in human β2-adrenergic receptor, $R^{3.50}$ contacts the $G\alpha_s$ subunit (Rasmussen et al., 2011).

As compared with $R^{3.50}$, the data on the requirement for $E/D^{3.49}$ in GPCR function are less clear-cut (Rovati et al., 2007). Some reports have found that mutating this residue compromises receptor function (Fraser et al., 1989; Hawtin, 2005) or has little effect on signaling (Lu et al., 1997), including in the CCR5 chemokine receptor (Lagane et al., 2005), while in other cases, mutating this residue has enhanced receptor activity (Rasmussen et al., 1999). Fewer studies have investigated the role of $Y^{3.51}$, and effects of mutations have been neutral (Lu et al., 1997; Zhu et al., 1994) or deleterious (Chen et al., 2001; Prado et al., 1997) for receptor signaling. With regard to $A^{3.53}$, as far as we are aware, the requirements at this position in GPCR's has not been addressed. However, a short stretch of residues including $V^{3.53}$ in rhodopsin was shown to be important for binding a C-terminal peptide of α_t of transducin (Acharya et al., 1997), and this residue interacted with a similar peptide in the Ops* (Scheerer et al., 2008) and metarhodopsin-II (Deupi et al., 2012) structures.

Residues in the $E/D^{3.49}R^{3.50}Y^{3.51}$ motif have also been studied to a limited extent for chemokine receptors, including CXCR4 (Doranz et al., 1999; Roland et al., 2003), CCR5 (Huttenrauch et al., 2002; Lagane et al., 2005), CXCR3 (Colvin et al., 2004), and CCR3 (Auger et al., 2002). Although their shared structures make generalizing tempting, the great diversity among GPCRs – and the available data – suggest that predicting roles for particular residues in the structure and function of a given receptor based on modeling from other GPCRs may be problematic. For example, the "ionic lock" has been shown to be absent and/or non-functional in structural and/or mutagenesis studies of multiple GPCRs (Cherezov et al., 2007; Jaakola et al., 2008; Rosenbaum et al., 2007; Warne et al., 2008), and in any case cannot form in the same way in the chemokine receptors, since these receptors lack $E^{6.30}$.

The data presented in this study have revealed that, just as for a number of other GPCRs, the residues in H3C of CXCR6, and also in CCR6, are important for receptor surface expression and/or ligand

Molecular Pharmacology Fast Forward. Published on August 27, 2015 as DOI: 10.1124/mol.115.099960
This article has not been copyedited and formatted. The final version may differ from this version.

binding and/or receptor signaling. In addition, we found cooperative effects among these residues. Of particular interest, we discovered that the functional consequences of altering H3C residues, singly and in combination, were highly cell-type dependent, and that these cell-type dependent effects correlated with selective differences in the receptors' use of $G_{i/o}$ proteins. These findings suggest that H3C not only contributes generally, as revealed by recent crystallographic data, to the strength of G protein binding, but also has a role in the promiscuity/selectivity of G protein use, even within a single subfamily of G proteins, and that receptor conformation governing this selectivity is affected by factors that are cell-type specific.

Materials and Methods

Cell Lines. HEK-293T, a human embryonic renal epithelial cell line stably expressing the large T antigen of SV40, and Jurkat clone E6-1, a human acute T cell leukemia cell line, were obtained from the American Type Culture Collection (Manassas, VA). HEK-293T cells were grown in Dulbecco's modified Eagle's medium (Life Technologies, Carlsbad, CA) and Jurkat clone E6-1 cells were grown in RPMI 1640 medium supplemented with 2 mM L-glutamine and 10% fetal bovine serum (FBS) at 37˚C in 5% CO_2.

Mutagenesis and Cloning of CXCR6 and CCR6 Receptors. cDNAs encoding wild type and mutant CXCR6 were constructed by polymerase chain reaction (PCR)-mediated mutagenesis using overlapping primers coding for the desired sequences using our wild type CXCR6 cDNA C3-9.1 in pCEP4 (Life Technologies) (Liao et al., 1997) as template. The wild type and mutant CXCR6 receptors were inserted in frame into the pEYFP-N1 vector (Clontech Laboratories, Palo Alto, CA) to encode CXCR6 C-terminal fusion proteins with yellow-green fluorescent protein (YFP). For each mutant receptor construct, four oligonucleotides (two flanking and two internal, overlapping primers) were used. In all the constructs the same sense (5'-GCTAGCAAGCTTGCCGCCACCATGGCAGAGCAT-3', containing the *Hin*dIII site, underlined) and antisense (5'-GACCGGTGGATCCCGTAACTGGAACATGCTGGT-3', containing a *Bam*HI site, underlined) primers were used. The internal primer sequences were: forward, 5'-TGCATCACTGTG**T**ATCGTTTCATTGTA-3' and reverse, 5'-TACAATGAAACGAT**A**CACAGTGATG

Molecular Pharmacology Fast Forward. Published on August 27, 2015 as DOI: 10.1124/mol.115.099960
This article has not been copyedited and formatted. The final version may differ from this version.

CA-3' for CXCR6-D126Y; forward, 5'-ACTGTGGATCGTT**A**CATTGTAGTGGTT-3' and reverse, 5'-AACCACTACAATG**T**AACGATCCACAGT-3' for CXCR6-F128Y; forward, 5'-GATCGTTTCATTG**C**AGTGGTTAAGGCC-3' and reverse, 5'-GGCCTTAACCACT**G**CAATGAAACGATC-3' for CXCR6-V130A; forward, 5'-TGCATCACTGTG**T**ATCGTTTCATTG**C**AGTGGTTAAGGCC-3' and reverse, 5'-GGCCTTAACCACT**G**CAATGAAACGAT**A**CACAGTGATGCA-3' for CXCR6-D126Y/V130A; forward, 5'-ACTGTGGATCGTT**A**CATTG**C**AGTGGTTAAGGCC-3' and reverse, 5'-GGCCTTAACCACT**G**CAATG**T**AACGATCCACAGT-3' for CXCR6-F128Y/V130A. Nucleotides differing from the wild-type sequence are shown boldface. Wild type and mutant CXCR6 sequences were also amplified using an alternative antisense flanking primer (5'-ATGTCTGGATCCCTATAACTGGAACATGCTGGT-3') and inserted into pCEP4 for the purpose of producing proteins that were not fused to YFP. cDNAs encoding wild type and mutant CCR6 were constructed by PCR-mediated mutagenesis using overlapping primers coding for the desired sequences with our wild type CCR6 cDNA F9-6.1 in pBKCMV (Life Technologies) (Liao et al., 1997) as template. The wild type and mutant CCR6 receptors were inserted in frame into the pEYFP-N1 vector to encode CCR6 C-terminal fusion proteins with YFP. For each mutant receptor DNA, four oligonucleotides (two flanking and two internal, overlapping primers) were used. In all the DNAs the same sense (5'-GCTAGCAAGCTTGCCGCCACCATGAGCGGGGAATCAATGAAT-3', containing the *Hin*dIII site, underlined) and antisense (5'-GACCGGTGGATCCCGCATAGTGAAGGACGACGC-3', containing a BamHI site, underlined) primers were used. The internal primer sequences were: forward, 5'-ATTAGCATG**T**CCGGTACATCGCC -3' and reverse, 5'-GGCGATGTACCGGT**A**CATGCTAAT-3' for CCR6-D142Y; forward, 5'-AGCATGGACCGGT**T**CATCGCCATTGTA-3' and reverse, 5'-TACAATGGCGATG**A**ACCGGTCCATGCT-3' for CCR6-Y144F; forward, 5'-GACCGGTACATCG**TG**ATTGTACAGGCG -3' and reverse, 5'-CGCCTGTACAAT**CA**CGATGTACCGGTC-3' for CCR6-A146V; forward, 5'-ATTAGCATG**T**ACCGGTACATCG**TG**ATTGTACAG-3' and reverse, 5'-CTGTACAAT**CA**CGATGTACCGGT**A**CATGCTAAT-3' for CCR6-D142Y/A146V; forward, 5'-AGCATGGACCGGT**T**CATCG**TG**ATTGTACAGGCG-3' and reverse, 5'-CGCCTGTACAAT**CA**CGATG**A**ACCGGTCCATGCT-3' for CCR6-Y144F/A146V. Nucleotides differing from the wild-type sequence are shown boldface. Plasmids

Molecular Pharmacology Fast Forward. Published on August 27, 2015 as DOI: 10.1124/mol.115.099960
This article has not been copyedited and formatted. The final version may differ from this version.

were isolated using the HiSpeed plasmid midi kit (Qiagen, Valencia, CA), and the sequences of the CXCR6, CXCR6-YFP and CCR6-YFP coding regions were determined in their entireties.

Transient Expression of Wild Type and Mutant CXCR6 and CCR6 Receptors in HEK-293T and Jurkat E6-1 Cell Lines. Cells were transfected with vector control, or DNAs encoding wild type and mutant CXCR6 and CCR6 using either FuGENE 6 transfection reagent (Roche Diagnostics, Indianapolis, IN) or the Amaxa nucleofector kit (Lonza, Gaithersburg, MD) according to the manufacturer's instructions. Amounts of DNA differed among experiments and are noted in the legends. In some experiments, quantities of DNAs for transfections were adjusted to achieve comparable levels of expression for wild-type and mutant receptors. Cells were harvested and used for analysis at either 48 hours (for FuGENE 6 transfections) or 24 hours (for Amaxa nucleofections).

Analysis of CXCR6 and CCR6 Surface Expression by Flow Cytometry. For most experiments, transfected cells were stained using a phycoerythrin (PE)-conjugated mouse IgG2b anti-human CXCR6 or CCR6 antibody (R&D Systems, Minneapolis, MN) and a similarly conjugated isotype control. For some experiments, transfected cells were incubated with affinity purified rabbit antibody that we raised against the 31 amino-terminal residues of CXCR6 by immunizing animals with a protein containing these residues fused to thioredoxin. After incubation with this antibody preparation or rabbit IgG as a control, cells were stained with PE-conjugated $F(ab')_2$ goat anti-rabbit IgG (Caltag Laboratories, Burlingame, CA). Incubations were done in phosphate buffered saline (PBS) containing 2% FBS and 0.1% NaN_3 at 4^oC for 30 minutes. After washing, stained cells were fixed in 1% paraformaldehyde and analyzed using a FACSCalibur flow cytometer (BD Biosciences, San Jose, CA) and FlowJo software (Tree Star, Ashland, OR).

Analysis of CXCR6 and CCR6 Expression by Confocal Microscopy. On the day before transfections, HEK-293T cells were plated onto poly L-lysine coated chambered cover-glass (Nalge Nunc International, Naperville, IL). Transfections with pcDNA3.1 (Life Technologies) and with DNAs encoding wild type and mutant CXCR6-YFP or CCR6-YFP fusion proteins were done using FuGENE 6. Forty-eight hours post-transfection the cells were stained with Hoechst 33482 (Molecular Probes, Inc., Eugene, OR) before being

Molecular Pharmacology Fast Forward. Published on August 27, 2015 as DOI: 10.1124/mol.115.099960
This article has not been copyedited and formatted. The final version may differ from this version.

analyzed on a laser scanning confocal microscope (Leica TCS-SP2; Leica Microsystems, GmbH, Mannheim, Germany). The Hoechst and YFP images were collected using a 63x oil immersion objective NA 1.32. Fluorochromes were excited using an Argon laser at 364 nm for Hoechst 33482 and 514 nm for YFP (Enterprise model 651, Coherent Inc., Santa Clara, CA). Hoechst 33482 emission was collected between 420-470 nm and YFP emission between 530-580 nm. The Hoechst 33482 and YFP images were collected separately and superimposed using Leica TCS-NT/SP software.

Ligand Binding Assays. Equilibrium dissociation constants (K_d) for binding of CXCL16 to CXCR6 wild type and mutant receptors as well as the receptor densities on transiently transfected HEK-293T and Jurkat E6-1 cells were determined by homologous displacement assays as described previously (Liao et al., 2002). Twenty-four hours after transfection, cells were harvested and suspended in Hanks' balanced salt solution (HBSS) containing 1% BSA, 25 mM HEPES and 0.02% NaN_3. Incubations were done in 200 µl containing 0.25 x 10^6 cells, 0.1 nM ^{125}I-CXCL16 (PerkinElmer Life Sciences, Boston, MA) and 0-100 nM unlabeled CXCL16 (PeproTech, Rocky Hill, NJ) for 45 minutes at room temperature before cells were spun through 10% sucrose in PBS. Cell-bound radioactivity was measured using a Cobra II series Auto-Gamma scintillation counter (Packard Instruments, Meriden, CT). Background counts were determined from samples containing 0.1 nM ^{125}I-CXCL16 in the absence of unlabeled ligand and cells, and were subtracted from each experimental value. The specific activity of radiolabeled CXCL16 ranged from 2230-2600 Ci/mmol depending on the lot; total counts were approximately 50,000-70,000 cpm; non-specific binding counts were approximately 150-300 cpm; and bound counts in the absence of unlabeled CXCL16 were approximately 5000-7000 cpm. Binding constants and receptor densities were calculated using LIGAND (P. Munson, Analytical Biostatistics, National Institutes of Health).

Chemotaxis Assays. Chemotaxis assays for HEK-293T cells were performed using a 48-well microchemotaxis chamber (NeuroProbe, Gaithersburg, MD) as described previously (Liao et al., 1999). Cells and chemokine were diluted in RPMI 1640 containing 25 mM HEPES, pH 8, and 1% BSA. Twenty-five thousand cells that had been transfected one day earlier were placed in the upper wells, at a

Molecular Pharmacology Fast Forward. Published on August 27, 2015 as DOI: 10.1124/mol.115.099960
This article has not been copyedited and formatted. The final version may differ from this version.

concentration of 5 X 10^5 cells/ml, over a polycarbonate membrane that contained 10 μm pores and that had been coated with 20 μg/ml rat tail collagen type IV. Lower wells contained CXCL16 in case of CXCR6 and CCL20 in case of CCR6 at 0-1000 ng/ml. Following incubation at 37°C in 5% CO_2 for 6 hours, cells adhering to the lower surface of the membrane were fixed and stained, and cells in five randomly chosen high-power (40x) fields were counted. Experimental values were averages from triplicate wells. Chemotaxis assays for Jurkat E6-1 cells were performed using Transwells (Costar, Cambridge, MA) as described previously (Liao et al., 2002). Cells and chemokine were diluted in RPMI 1640 containing 10 mM HEPES, pH 8, and 0.5% BSA. One million cells that had been transfected one day earlier were placed in the inserts, at a concentration of 1 X 10^7 cells/ml, on a membrane containing 5 μm pores and the inserts were placed in wells containing 0-500 ng/ml CXCL16 or 100 ng/ml CCL20. Following incubation at 37°C in 5% CO_2 for 3 hours, cells in the lower wells were collected and counted using a Vi-CELL analyzer (Beckman Coulter, Miami, FL). In some experiments, cells were pretreated for 3 hours at 37°C with 500 ng/ml pertussis toxin (Calbiochem, San Diego, CA).

Measuring Polymerization of F-Actin. Assays for actin polymerization were performed as described previously (Liao et al., 2002). Transfected cells were incubated at 2.5 x 10^6 cells/ml at 37°C for 20 min in HBSS containing 10 mM HEPES and 1% FBS before the addition of 2.5 μg/ml CXCL16. After 5, 10, 15, 30, and 60 seconds, cells were fixed and stained in 4% paraformaldehyde, 0.5% saponin, 1.7 μg/ml phalloidin and 132 nM Alexa Fluor 488 phalloidin (Molecular Probes) for 10 minutes on ice, and washed 3 times with PBS containing 0.1% saponin, 1% BSA and 0.05% NaN_3. Stained cells were resuspended in PBS and phalloidin fluorescence was measured on a FACScalibur cytometer (BD Biosciences). Results for each sample are expressed as increase in mean fluorescence intensity as compared with cells that had been fixed and stained without addition of chemokine.

Measuring Calcium Flux. Calcium flux assays were done using two methods as described previously (Liao et al., 1995; Rabin et al., 1999). All manipulations for assaying calcium flux were done in HBSS containing Ca^{2+}/Mg^{2+}, 20 mM HEPES, pH 7.4 and 1% FBS. For most experiments, measurements were

Molecular Pharmacology Fast Forward. Published on August 27, 2015 as DOI: 10.1124/mol.115.099960
This article has not been copyedited and formatted. The final version may differ from this version.

made using a dual excitation ratio fluorescence spectrometer (Photon Technology International, Monmouth Junction, NJ). For these measurements, cells were loaded with 2 μM Fura-2/AM (Molecular Probes) for 40 minutes at 37°C, washed, and kept at 37°C until being used for assays. Measurements were done at 0.5 x 10^6 cells/ml with excitation alternately at 340 and 380 nm and emission at 510 nm using an integration time of 0.5 seconds, and the ratios of the emitted signals obtained at the two excitation wavelengths were plotted vs. time. For some experiments, measurements were made using a BD LSR II Flow Cytometer (BD Biosciences). For these measurements, transfected cells were loaded with 5 μM indo-1/AM in 0.2% Pleuronic F-127 (Molecular Probes) for 45 minutes at 37°C, washed, and kept at room temperature until just before being assayed, when they were warmed to 37°C. Data were collected before and after addition of CXCL16. Excitation was at 325 nm and fluorescence was recorded at 405 and 525 nm for calcium-bound and free probes, respectively, vs. time. The data were analyzed using FlowJo software (Tree Star). Cells used in these experiments had been shown to have equal levels of surface expression of wild-type/mutant CXCR6 proteins by antibody staining (see Supplemental Figure 1) and electronic gating was done to analyze only cells that were YFP^+. The percent cells responding was calculated based on numbers of cells having a ratio of violet/blue above a threshold that was set at the 95th percentile for the cells collected before the addition of CXCL16 (Rabin et al., 1999).

Molecular Modeling. The inactive dimeric form of CXCR4 was chosen as a template for modeling CXCR6 by SwissModel (Kiefer et al., 2009). The dimer model was inserted into a POPC membrane, solvated, and ions added for charge equilibration using tools within visual molecular dynamics (VMD) (Humphrey et al., 1996). Substitutions were made to create the mutant structures for CXCR6 (D126Y, F128Y, V130A, D126Y-V130A, F128Y-V130A). Simulations were performed using the CHARMm force field in NAMD (Phillips et al., 2005). Each approximately 180,000-atom system was minimized over 200,000 conjugate gradient steps, warmed from 40 K to 310 K in 10 K increments over 5000 steps each, and then equilibrated with a 1 fsec time-step for 30 nsec under isothermal-isobaric conditions of 310 K and 1 atm using periodic boundary conditions in a rectangular prism of approximate dimensions 110 by 160 by

Molecular Pharmacology Fast Forward. Published on August 27, 2015 as DOI: 10.1124/mol.115.099960
This article has not been copyedited and formatted. The final version may differ from this version.

100 Å. Snapshots of the last 20 nsec of each simulation were taken every 100 psec for each protomer for further analysis. The counts of the pairwise hydrogen bonds and neighboring contacts from LigPlot (Phillips et al., 2005), the secondary structure assignments from STRIDE (Frishman and Argos, 1995), and the metrics from the TRAJELIX module of Simulaid (Mezei, 2010) were averaged over these 200 snapshots and compared with Bonferroni-corrected *t* tests.

Knockdown of G Protein α-Subunits by siRNA. SmartPool control siRNAs (Catalogue number D-001810-10-0005) and siRNAs specific for $G\alpha_{i1}$ (L-010404-00-0005), $G\alpha_{i2}$ (L-003897-00-0005), $G\alpha_{i3}$ (L-005184-00-0005), and $G\alpha_{o}$ (L-009486-00-0005) were obtained from Dharmacon (Lafayette, CO). The siRNA sequences for these genes are available upon request. Each siRNA sample was resuspended in 250 µl of buffer as per the manufacturer's instructions to give 20 µM stock solutions. Transfections of Jurkat E6.1 cells were performed with the amaxa nucleofector device and of HEK-293T cells with X-tremeGENE siRNA transfection reagent (Roche Diagnostics). In all cases, cells were transfected with 4 µg of plasmid DNA encoding CXCR6-WT or mutant receptor together with 15 µL of the appropriate siRNA solution. Transfected cells were incubated at 37°C, 5% CO_2 for 72 hours before being analyzed. Percent inhibition of peak ratio fluorescence in calcium flux assays using a fluorescence spectrometer in response to CXCL16 was calculated for cells expressing wild-type and mutant CXCR6 proteins and transfected with various $G\alpha_{i/o}$ siRNAs as compared with control siRNAs.

Western Blotting. Cells were lysed on ice for 1 hour in chilled lysis buffer (50 mM Tris HCl, pH 8.0, 150 mM NaCl, 1 mM EDTA, and 2% Triton X-100) containing 1:200 protease inhibitor cocktail (Sigma-Aldrich, St. Louis, MO). Cellular lysates were centrifuged at 12,000 x g for 10 min at 4°C and supernatants were collected after centrifugation. Protein content was quantified using the Micro BCA Protein assay (Pierce Biotechnology, Inc., Rockford, IL) according to the manufacturer's guidelines with BSA as a standard. Samples were prepared for SDS-PAGE by boiling at 100°C with 2 x Laemmli Sample buffer (Bio-Rad Laboratories, Hercules, CA) plus 8 M urea. Ten µg of cellular proteins were analyzed by Western blotting as described previously (Foley et al., 2010).

Molecular Pharmacology Fast Forward. Published on August 27, 2015 as DOI: 10.1124/mol.115.099960
This article has not been copyedited and formatted. The final version may differ from this version.

Isolation of RNA, Synthesis of cDNA, and Semi-Quantitative Real-Time RT-PCR. Total cellular RNA was isolated using the Trizol reagent (Life Technology). Real-time RT-PCR was performed with 50 ng of RNA using SuperScript One Step RT-PCR kit (Life Technology). Inventoried primer and probe sets (FAM/MGB-labeled) were purchased from Applied Biosystems (Foster City, CA). Primer/probe sequences are available upon request. Real-time PCR analysis was performed on samples in duplicate using an ABI 7900 Sequencer System (Applied Biosystems). Concentrations of input RNA and primers were adjusted to assure that threshold cycles were within the exponential phase of amplification. Results were normalized based on the values for *GAPDH* mRNA, detected using TaqMan *GAPDH* Control reagents (Applied Biosystems).

Statistical Analysis. The mean and standard error of the mean are expressed for values obtained from the number of independent experiments indicated. Statistically significant differences between two groups were determined using Student's *t*-test and expressed as $P < 0.05$ (*), $P < 0.01$ (**), $P < 0.001$ (***) and $P < 0.0001$ (****). All statistical analysis was performed using GraphPad Prism software (GraphPad Software, San Diego, CA).

Results

Structure and Mutagenesis of CXCR6. Fig. 1A depicts the sequence of CXCR6, and in Fig. 1B are shown the H3C sequences of the human chemokine receptors, where it can be seen that CXCR6 is the only receptor with F128 in place of Y128 and only one of four receptors with a replacement of A130 (V130 in CXCR6). To investigate the function of the H3C residues in CXCR6, we produced CXCR6 mutants in which the non-canonical F128 and V130 were replaced with the canonical Y and A, respectively, singly and in combination as well as mutants replacing the canonical D126 with Y, and containing either V130 or A130 (Fig. 1C). Based on previous studies of the α_{1B}-adrenergic receptor (Scheer et al., 1997), the substitution of the polar Y in place of the D126 might not be expected to be as disruptive – and therefore potentially more informative – as compared, for example, with introducing a highly hydropathic residue.

Molecular Pharmacology Fast Forward. Published on August 27, 2015 as DOI: 10.1124/mol.115.099960
This article has not been copyedited and formatted. The final version may differ from this version.

We also replaced the canonical amino acid residues in CCR6, which among other receptors has greatest sequence homology with CXCR6, with the non-canonical residues found in CXCR6 (Fig. 1D).

Mutants of CXCR6 Containing D126Y Accumulate Intracellularly. HEK-293T cells were transfected with DNAs encoding the wild type and mutant CXCR6 receptors fused at their C-termini with YFP. The fluorescent signals produced by YFP after transfections with equal amounts of each of the DNAs were equivalent (Fig. 2A), reflecting close to equal expression of each of the fusion proteins. However, when transfected cells were stained with either a mouse monoclonal (Fig. 2B) or a rabbit polyclonal anti-human-CXCR6 antibody (data not shown), mutants containing Y in place of D126 showed lower surface expression as compared with wild type or other mutant receptors. Similar results were obtained after transfection of Jurkat E6-1 cells (data not shown). Together, these data suggested that mutants containing D126Y were preferentially distributed intracellularly as compared with the other receptors. This was verified by confocal microscopy of cells expressing CXCR6-YFP fusion proteins (Fig. 2C). Equal levels of surface expression for the D126Y and wild type receptors could be achieved by manipulating the amounts of DNAs used for transfections, as in the examples shown in Supplemental Figure 1, which was done for some experiments in order to simplify comparisons of receptor signaling (see below). The data shown below are from experiments using CXCR6-YFP fusion proteins. All of the functional studies (except for knockdown of G protein α-subunits by siRNA, see below) using HEK-293T cells and some (flow cytometry, chemotaxis, calcium flux, and ligand binding assay, see below) of the studies using Jurkat E6-1 cells were also performed using non-fusion CXCR6 proteins and results with fusion and non-fusion proteins were similar (data not shown).

Binding of CXCL16 to cells transfected with DNAs encoding wild type or mutants of CXCR6 as part of YFP fusion proteins was analyzed using the extracellular chemokine domain (N49-P137) of CXCL16 in homologous displacement assays. Amounts of DNAs transfected were adjusted to yield cells expressing equivalent numbers of each of the receptors as determined by antibody staining, as in the examples shown in Supplemental Figure 1. Using cells that were either not transfected or transfected with vector alone (pEYFP-N1) gave no counts above background. As shown in Supplemental Figure 2,

Molecular Pharmacology Fast Forward. Published on August 27, 2015 as DOI: 10.1124/mol.115.099960
This article has not been copyedited and formatted. The final version may differ from this version.

displacement curves suggested a single high affinity site on cells expressing each of the receptors. Wild-type CXCR6 and the V130A and F128Y/V130A mutants showed similar K_d's of approximately 1.6 nM. By contrast, the mutants with Y in place of D126 (D126Y and D126Y/V130A) showed lower K_d's of approximately 0.9 nM and the F128Y mutant showed a higher K_d of approximately 3.5 nM (Table 1). Although the differences in the K_d's for these latter receptors vs. wild-type CXCR6 are modest, they were found reproducibly over multiple experiments ($P < 0.001$).

Non-canonical to Canonical Mutations Diminish the Activity of CXCR6 Expressed on HEK-293T Cells. To characterize their functional capabilities, we analyzed the mutant vs. wild-type CXCR6 receptors in assays for chemotaxis, calcium flux and actin polymerization. As shown in Supplemental Figure 3, we found a bell-shaped response for migration of transfected HEK-293T cells expressing wild type CXCR6 to increasing concentrations of chemokine, with the maximum response at 125 ng/ml of CXCL16. Using this concentration of CXCL16, we found, as shown in Fig. 3A, that cells expressing mutant receptors D126Y and D126Y/V130A migrated at close to wild-type levels. Chemotaxis was modestly impaired for mutant receptors V130A and F128Y/V130A (P <0.01 vs. wild-type), and significantly impaired for mutant receptor F128Y (P <0.001). It is noteworthy that the two mutants containing D126Y functioned at close to wild-type levels despite, in these experiments, lower surface expression (Fig. 2B), consistent with the mutants' higher affinities for CXCL16. Analogous to the results for ligand binding, replacing Val130 with the canonical Ala "corrected" the function of the single F128Y mutant toward the wild-type level (P < 0.001 for F128Y/V130A vs. F128Y). Given these findings, it was possible that diminished activity in chemotaxis for mutant F128Y simply reflected an isolated defect in ligand binding. If so, it should have been possible to reach wild-type levels of function at higher concentrations of CXCL16. However, as shown in the right panel in Fig. 3A, not only was the dose response of the F128Y mutant shifted to the right, but also the activity of the F128Y mutant did not reach the maximum mediated by the wild-type receptor no matter the concentration of CXCL16, consistent with both diminished affinity for ligand and defective signaling in the F128Y mutant.

Molecular Pharmacology Fast Forward. Published on August 27, 2015 as DOI: 10.1124/mol.115.099960
This article has not been copyedited and formatted. The final version may differ from this version.

Although chemotaxis is typically the most sensitive assay for chemokine receptor activity, signaling could also be evaluated independently of differences in affinities for ligand using assays of filamentous actin (F-actin) polymerization and calcium flux, which do not show bell-shaped dose responses to chemokine and can use saturating concentrations of ligand. Although chemotaxis, actin polymerization, and calcium flux require activation of G proteins, the activities differ in their dependence on signaling pathways further downstream (reviewed in (Wu et al., 2000)). For CXCL16-induced polymerization of F-actin in the transfected HEK-293T cells, as shown in Fig. 3B, signaling was most decreased for the F128Y mutant (P <0.01 vs. the wild-type receptor), whereas signaling through the other receptors was only slightly diminished, and function of F128Y/V130A was significantly improved compared with F128Y (P <0.05).

For measuring calcium flux, two assays were employed, including one using flow cytometry, which allowed us to analyze calcium signals specifically on the receptor-expressing, YFP^+ cells. For the calcium experiments, the amounts of the DNAs used for transfection were manipulated so that all receptors were expressed at nearly equal levels on the cell surface as determined by antibody staining, as in the examples shown in Supplemental Figure 1. In both types of calcium assays (Fig. 3C and Supplemental Figure 4), all mutant receptors signaled as well as the wild type with the exception of the F128Y mutant (P <0.01 vs. the wild-type receptor) and function of F128Y/V130A was significantly improved compared with F128Y (P <0.01). It is likely that the calcium assays did not reflect the modest effects found for the V130A and F128Y/V130A mutants in chemotaxis due to the differences in the assays' sensitivities to changes in receptor activity. In dose response data not shown, we found a lower EC_{50} for the D126Y mutant (63 ng/ml) as compared with the wild-type receptor (86 ng/ml), consistent with the D126Y mutant's lower K_d. However, equal signaling by the mutants containing D126Y and the wild-type receptor under conditions of equal levels of surface expression and saturating concentrations of CXCL16 suggest that these mutants did not have a significantly enhanced ability to signal independently of their increased affinity for ligand. On the other hand, taken together, our data demonstrate that when assayed in HEK-293T cells, changing the non-canonical F128 to the canonical Y led to decreased ligand binding and an

Molecular Pharmacology Fast Forward. Published on August 27, 2015 as DOI: 10.1124/mol.115.099960
This article has not been copyedited and formatted. The final version may differ from this version.

additional, proximal defect in signaling, both of which could be rectified by replacing the non-canonical V130 with the canonical A.

CXCR6-D126Y has Impaired Activity When Expressed in Jurkat E6-1 Cells. Because CXCR6 is expressed on human $CD4^+$ T cells, we evaluated the CXCR6 proteins in Jurkat E6-1 cells, whose parent cell line was derived from a $CD4^+$ T cell leukemia. As shown in Supplemental Figure 5, the K_d measurements for the wild-type and mutant receptors were generally lower in the Jurkat E6-1 cells as compared with HEK-293T cells. Two findings were of interest in these experiments: 1) Unlike in the HEK-293T cells, the F128Y mutant showed a K_d for CXCL16 that was not significantly different from the wild-type receptor; and 2) similar to what we found in the HEK-293T cells, mutants containing D126Y showed a K_d of approximately one-half the wild-type value (Table 1).

As we had done in the HEK-293T cells, we analyzed the CXCR6 proteins in transfected Jurkat E6-1 cells in assays for chemotaxis, F-actin polymerization and calcium flux (Fig. 4). As shown in Supplemental Figure 6, we established that 62.5 ng/ml was the concentration of CXCL16 producing the highest level of migration of cells expressing the wild-type CXCR6 when assayed on Jurkat E6-1 cells in the Transwell apparatus, and this was the concentration used for the comparisons displayed in Fig. 4A (left panel). For the chemotaxis and calcium assays, the amounts of the DNAs used for transfection were adjusted to give approximately equal levels of surface expression of the CXCR6 proteins, as in the examples shown in Supplemental Figure 1. The chemotaxis experiments demonstrated that activities of the V130A and D126Y/V130A mutants were modestly reduced as compared with the wild-type receptor. In contrast, and despite it's lower K_d for CXCL16, the D126Y mutant showed markedly reduced activity ($P < 0.001$ vs. the wild-type receptor). Just as we had seen for the F128Y mutant in the HEK-293T cells, replacing the non-canonical V130 with the canonical A in the D126Y/V130A mutant partly restored activity. In addition, the F128Y/V130A double mutant showed a wild-type level of activity, rectifying the modest deficiency of the V130A mutant. We evaluated the dose response curve for the D126Y mutant vs. wild-type CXCR6 in the Jurkat E6-1 cells. As shown in Fig. 4A (right panel), although the peak activity for the D126Y mutant was at a lower concentration of CXCL16 as compared with the wild-type receptor,

Molecular Pharmacology Fast Forward. Published on August 27, 2015 as DOI: 10.1124/mol.115.099960
This article has not been copyedited and formatted. The final version may differ from this version.

at no concentration of CXCL16 did the activity of the D126Y mutant reach the maximum demonstrated by the wild-type CXCR6. These data are consistent with both a lower K_d for CXCL16 and a signaling defect for the D126Y mutant as compared with wild-type CXCR6 in Jurkat E6-1 cells.

Analogous to the chemotaxis data, assays for F-actin polymerization in the Jurkat E6-1 cells (Fig. 4B) showed the most dramatic reduction in activity for the D126Y mutant (P <0.01 vs. the wild-type receptor). There was also a suggestion of a "corrective" effect of the V130A substitution in the D126Y/V130A mutant. The calcium assays at saturating doses of CXCL16, as shown in Fig. 4C, also gave results similar to what we saw for chemotaxis. All mutant receptors signaled as well as the wild type with the exception of the D126Y mutant (P <0.01 vs. the wild-type receptor) and function of D126Y/V130A was significantly improved compared with D126Y (P <0.05). Together, these data demonstrate that similar to what we found in the HEK-293T cells, abnormalities in receptors with single amino acid changes were minimized in the receptors with a second mutation, but that in contrast to what we found in HEK-293T cells, the defects in ligand binding and signaling for the F128Y mutant were undetectable or much less pronounced, and that despite its higher affinity for CXCL16, the D126Y mutant showed a significant, global signaling defect in these cells.

Computational Modeling of CXCR6. To investigate the effects of mutations in the H3C on the structure of CXCR6, we chose the crytallographic structure of the inactive dimeric form of CXCR4 (Wu et al., 2010) as a template for modeling using SwissModel. This model of CXCR6 consists of 265 residues from position 26 to 290 in presumably an inactive conformation. No voids or other anomalies developed over the course of simulation. After controlling for global translation and rotation, the C-alpha RMSD from the initial model showed that the systems were in an equilibrium state for the last 20 nsec of the simulations (Fig. 5A). The following analysis considers the systems in these equilibrated states only.

The gross structural differences among the simulations of mutant versus wild-type receptors were concentrated in the N-terminus of helix four. Mutations affected both the length (Fig. 5B, E) of helix four and its rotation (Fig. 5C, F) about its long axis. Length and rotation of the other helices were unaffected by the various mutations (data not shown). F128Y, which showed compromised function in HEK-293T cells,

Molecular Pharmacology Fast Forward. Published on August 27, 2015 as DOI: 10.1124/mol.115.099960
This article has not been copyedited and formatted. The final version may differ from this version.

and D126Y, which showed compromised function in Jurkat E6-1 cells, demonstrated shortening and rotation of helix four. In the double mutants in which the V130A mutation restored activity, the length of helix four was increased and degree of rotation was reduced, bringing the structure back toward wild-type.

We also looked for local perturbations near the mutated residues (D126, Y128, and V130). A strong electrostatic and hydrogen bond network formed involving helix six (S229) and helix four (K143) via the D126–R127 salt bridge in helix three in WT, V130A, and F128Y/V130A (Fig. 5D, E). Disruptions of this network in the simulations were also associated with loss of CXCR6 function in either HEK-293T or Jurkat E6-1 cells. In these simulations, some of the differences among the structures are evident in only one of the two protomers. In D126Y, helix four frayed as much as six residues or two turns because of the increased steric bulk and different electrostatics associated with Y126, which disrupted the native interactions that coil the helix (Fig. 5B, E). This was also reflected in the widely varying rotation angle of helix four in D126Y (Fig. 5C). The additional V130A mutation in D126Y/V130A allowed helix four to return towards its native length and rotation because the smaller bulk of A130 compensated for the larger bulk of Y126 (Fig. 5B - E).

Effects on rotation of helix four are greatest for mutations at either F128 or V130. The mutations at these positions induced a counter-clockwise rotation of about 20° in helix four (Fig. 5 C, D, and F), which rotated T146 (helix four) towards the dimer interface, V150 (helix four) away from the dimer interface, and K143 (helix four) and W147 (helix four) inwards towards D126 (Fig. 5D and F). Again, some of the differences among the structures are evident in only one of the two protomers. For the V130A mutant, we speculate that this rotation was due to the void introduced by the loss of the hydrophobic methyl groups at A130, inducing helix four to rotate inwards to fill the space. Even though helix four rotated, it retained its wild-type length in both V130A and F128Y/V130A (Fig. 5B). This may have been because interactions of D126 with K143 (helix four) in both mutants, and F128 with V150 (helix four) in the opposite protomer in the V130A mutant remained intact or were even strengthened (Fig. 5D).

In a different but complimentary mechanism, the F128Y mutation introduced a polar group into the dimer interface near the hydrophobic V150 (helix four) in the opposite protomer. The resulting

Molecular Pharmacology Fast Forward. Published on August 27, 2015 as DOI: 10.1124/mol.115.099960
This article has not been copyedited and formatted. The final version may differ from this version.

unfavorable interaction may have lead to the rotation of helix four, which placed T146 (helix four) in proximity to the mutated Y128 in the opposite protomer, where the two residues could potentially interact via a hydrogen bond. However, despite their proximity, a hydrogen bond does not form in F128Y because of steric interferences with V130. These interferences may also be responsible for the diminished interaction between D126 and R127 and the fraying of the N-terminus of helix four. The greater plasticity in the mutation site afforded by A130 in F128Y/V130A eased these steric effects and, as a result, the interaction between D126 and R127 was restored, the length of helix four returned to normal, and a hydrogen bond formed between Y128 and T146 (helix four) (Fig. 5D, F).

Differential Coupling of CXCR6 Wild-type and Mutant Receptors to $G\alpha_{i/o}$ Proteins. In trying to understand the cell type-specific differences in the behaviors of the various mutants, we considered whether these could be due to differences in the mutants' abilities to couple to particular species of G proteins together with differences in the abundances of G protein species between the cell lines. In order to make direct quantitative comparisons among the different G protein α-subunit mRNAs by RT-PCR, we established that the corresponding sets of primers and probes showed equal efficiencies of amplification, using as substrates plasmids containing each of the Gα cDNA sequences (Foley et al., 2010). We compared levels of mRNAs for multiple Gα subunits in HEK-293T cells versus Jurkat E6-1 cells (Supplemental Figure 7A). Because all activities of CXCR6 could be inhibited by pertussis toxin (Supplemental Figure 8), we focused our analyses on $G\alpha_{i/o}$ proteins, and we compared levels of $G\alpha_{i2}$, $G\alpha_{i3}$, and $G\alpha_{o}$ subunits in these cell lines by Western blotting (Supplemental Figure 7B). Of note, all reagents that we used for $G\alpha_{o}$ did not discriminate between $G\alpha_{oA}$ and $G\alpha_{oB}$. Western blotting was not done for $G\alpha_{i1}$ due to the lack of a $G\alpha_{i1}$-specific antibody. Taken together, our data in Supplemental Figure 7 showed that $G\alpha_{i1}$ mRNA was more abundant in HEK-293T cells, whereas, $G\alpha_{i2}$ protein was more abundant in Jurkat E6-1 cells. Nonetheless, the mRNA data suggested that $G\alpha_{i2}$ was the most abundant of the $G\alpha_{i/o}$ subunits in both cell lines. Amounts of $G\alpha_{i3}$ and $G\alpha_{O}$ proteins in the two cell lines were similar.

Molecular Pharmacology Fast Forward. Published on August 27, 2015 as DOI: 10.1124/mol.115.099960
This article has not been copyedited and formatted. The final version may differ from this version.

In order to analyze G protein use by the various receptors, we used siRNA-mediated knockdown of individual $G\alpha_{i/o}$ subunits. Our prediction was that if a mutant receptor's compromised function were due to selective loss in the ability to couple to a particular $G\alpha$ subunit, then knockdown of that subunit would have less of an impact on signaling as compared with the wild-type receptor. Western blotting, and RT-PCR for $G\alpha_{i1}$ mRNA, demonstrated that we achieved selective knockdown of $G\alpha_{i/o}$ subunits in HEK-293T cells (Supplemental Figures 9-10) and Jurkat E6-1 cells (Supplemental Figures 11-12).

In HEK-293T cells (Fig. 6) the calcium signal produced through the wild-type receptor was inhibited significantly by knockdown of each of the $G\alpha_{i/o}$ subunits. It is notable that summing each of the % inhibitions totaled more than 100, suggesting the possibility of cooperative effects among G proteins. In these cells, F128Y was the mutant showing the greatest functional compromise, and the pattern of inhibition for this mutant differed from the wild-type in showing loss of dependence on $G\alpha_o$, consistent with a diminished ability of the F128Y mutant to use G_o proteins. For F128Y/V130A, which showed return to near-wild-type function, dependence on $G\alpha_o$ was restored and the pattern now resembled that of the wild-type receptor. The proteins containing the D126Y mutation also showed a pattern that differed from wild-type, with generally diminished effects of knockdown of individual $G\alpha_{i/o}$ subunits. However, in this case, given the ability of D126Y mutants to function at wild-type levels in HEK-293T cells even where their surface expression was reduced, we interpret the pattern to result from the D126Y receptors' ability to use at least some of the $G_{i/o}$ proteins more efficiently than wild-type. The V130A single mutant showed the wild-type pattern, consistent with the limited effect of this mutation alone on receptor function.

In the Jurkat E6-1 cells (Fig. 7), just as in the HEK-293T cells, the knockdown data suggested that the wild-type receptor was using all the $G_{i/o}$ proteins, except for G_{i1} (Fig. 7), consistent with the very low level of $G\alpha_{i1}$ mRNA in these cells (Supplemental Figure 7A). The function of the F128Y-containing proteins was not impaired in Jurkat E6-1 cells, and in these cells the pattern of inhibition after knockdown of the $G\alpha_{i/o}$ subunits was the same as wild-type. For example, by contrast with the results in HEK-293T cells, the F128Y mutants showed the wild-type pattern of use for $G\alpha_o$. The D126Y single mutant was the

Molecular Pharmacology Fast Forward. Published on August 27, 2015 as DOI: 10.1124/mol.115.099960
This article has not been copyedited and formatted. The final version may differ from this version.

receptor with the most compromised function in the Jurkat E6-1 cells, and the pattern of inhibition was very different from wild-type. In particular, the limited dependence on $G\alpha_{i2}$ likely reflected a diminished ability to use G_{i2} proteins, which would be expected to have a significant effect on receptor activity in Jurkat E6-1 cells. In the double mutant, D126Y/V130A, which showed a return to near-wild-type function, the pattern of inhibition in Jurkat E6-1 cells resembled the pattern for the wild-type receptor.

Canonical to Non-canonical Mutations Diminish the Activity of CCR6 When Expressed on HEK-293T or Jurkat E6-1 Cells. In order to compare our results from mutations in CXCR6 with those from a related receptor displaying the canonical chemokine receptor sequences, we created mutations in CCR6, the receptor to which CXCR6 is most closely related. These mutations included D142Y, and additional changes to replace CCR6 sequences with those found in CXCR6, including replacing Y144 with F and A146 with V. HEK-293T cells transfected with DNAs encoding the wild type and mutant CCR6 receptors fused at their C-termini with YFP showed similar fluorescent signals produced by YFP, reflecting close to equal expression of each of the fusion proteins (Supplemental Figure 13A). However, when transfected cells were stained with either a mouse monoclonal (Supplemental Figure 13B) or a rabbit polyclonal anti-human-CCR6 antibody (data not shown), mutants containing Y in place of D142 showed lower surface expression as compared with wild type or other mutant receptors. Similar results were obtained after transfection of Jurkat E6-1 cells (data not shown). Together, these data suggested that just as for CXCR6 the CCR6 mutants containing D126Y were preferentially distributed intracellularly as compared with the other receptors. This was verified by confocal microscopy of HEK-293T cells expressing CCR6-YFP fusion proteins (Supplemental Figure 13C).

To characterize their functional capabilities, we analyzed the mutant vs. wild type CCR6 receptors in assays for chemotaxis and calcium flux. For HEK-293T cells, in experiments not shown, we found a bell-shaped dose response for migration of transfected cells expressing wild-type CCR6 to the CCR6 ligand, CCL20, with the maximum response at 100 ng/ml. Using this concentration of CCL20 in the lower wells, we found, as shown in Fig. 8A, that chemotaxis was modestly impaired for mutant receptors D142Y ($P < 0.01$ vs. wild type), and Y144F ($P < 0.05$ vs. wild type). Replacing canonical A146 with the non-canonical

Molecular Pharmacology Fast Forward. Published on August 27, 2015 as DOI: 10.1124/mol.115.099960
This article has not been copyedited and formatted. The final version may differ from this version.

V partially "corrected" the function of the single D142Y mutant toward the wild-type level ($P < 0.01$ for D142Y/A144V vs. D142Y) and showed a similar trend in correcting the Y144F mutant.

For the calcium flux experiments in HEK-293T cells, the amounts of the DNAs used for transfection were manipulated so that all receptors were expressed at nearly equal levels on the cell surface as determined by antibody staining. As shown in Fig. 8B, all mutant receptors, including the Y144F mutant, signaled similarly to the wild type with the exception of receptors containing the D142Y mutation and D142Y/A146V ($P < 0.001$ vs. the wild-type receptor), although the D142Y/A146V mutant functioned significantly better than the D142Y single mutant. Our data demonstrate that changing the canonical D142 in CCR6 to Y led to defective signaling, which could be rectified by replacing the canonical A146 with V.

We also analyzed the CCR6 proteins in transfected Jurkat E6-1 cells. For the chemotaxis and calcium assays, the amounts of the DNAs used for transfection were adjusted to give approximately equal levels of surface expression of the CCR6 proteins. The chemotaxis experiments demonstrated that activities of the receptors containing the D142Y mutation were significantly reduced as compared with the wild-type receptor (Fig. 8C, $P < 0.01$). Just as we saw for the D142Y mutant in the HEK-293T cells, replacing the canonical A146 with V partly restored the activity of the D142Y mutant ($P < 0.001$). In addition, the Y144F/A146V double mutant showed a wild-type level of activity, rectifying the deficiencies of Y144F mutant ($P < 0.01$). The calcium assays using the Jurkat E6-1 cells and saturating doses of CCL20, as shown in Fig. 8D, also gave results similar to what was found for chemotaxis. The poorest response was shown by the receptors containing D142Y ($P < 0001$ vs. wild-type) with partial "correction" in the D142Y/A146V mutant ($P < 0.01$) and close to wild-type responses shown by the other mutants.

Discussion

Recent structural studies have suggested that the third transmembrane helix is particularly critical in the structure and function of class A rhodopsin-like receptors, containing residues that contact receptor ligands as well as G proteins (Venkatakrishnan et al., 2013). Our studies were undertaken to investigate the roles of the atypical sequences in H3C on the cytoplasmic face of CXCR6 in order to understand better the

Molecular Pharmacology Fast Forward. Published on August 27, 2015 as DOI: 10.1124/mol.115.099960
This article has not been copyedited and formatted. The final version may differ from this version.

functions of the H3C sequences in CXCR6 and chemokine receptors generally. Our analysis of point mutations in H3C of CXCR6 is summarized in Table 1.

For the CXCR6 D126Y mutant, and the F128Y mutant in HEK-293T cells, we found effects on CXCL16 binding. For E/D$^{3.49}$ (D126 in CXCR6), previously published data have also shown that mutations can affect agonist binding (Fraser et al., 1989; Hawtin, 2005; Li et al., 2001; Rovati et al., 2007). Our results are consistent with allosteric interactions between H3C, which contains residues contacting G proteins, and the receptors' ligand-binding sites. These interactions are reflected in the long-recognized cooperative effects between binding of extracellular ligand and G protein due to the formation of a ternary complex (De Lean et al., 1980) and the findings that binding of the Gα subunit peptides or G proteins stabilize the active conformation of the receptor and allow for high affinity ligand binding (Hamm et al., 1988; Whorton et al., 2007). Bidirectional coupling between the G protein- and ligand-binding sites has been further highlighted by recent results for the structure of the α_{2A} adenosine receptor bound by an inverse-agonist antibody (Hino et al., 2012).

For chemokine binding and/or receptor function, the deleterious effects of the F128Y mutation in CXCR6 in HEK-293T cells were nullified by replacing V130 with A, and in Jurkat E6-1 cells, the modest defect in chemotaxis in the V130A mutant was also eliminated in the F128Y/V130A double mutant. Similarly, in CCR6, deleterious effects of the Y144F mutation were eliminated in the Y144F/A146V double mutant. These findings suggest matching of the non-canonical and canonical sequences in the H3C of these chemokine receptors to provide the optimal conformations. In addition, we found that replacing V130 with A in CXCR6 mitigated the deleterious consequences of replacing the canonical D126 with Y in Jurkat E6-1 cells, and replacing A146 with V in CCR6 had a similar effect on mitigating the effects of the D142Y mutation.

Our molecular modeling was based on the structure of CXCR4 in an inactive conformation (Wu et al., 2010). We chose to model CXCR6 on the CXCR4 data because, as another CXC chemokine receptor, it shows homology in sequence, structure, and function. In addition, the solved CXCR4 structure is

Molecular Pharmacology Fast Forward. Published on August 27, 2015 as DOI: 10.1124/mol.115.099960
This article has not been copyedited and formatted. The final version may differ from this version.

dimeric. Although a general, functional role for dimerization among class A GPCRs remains unclear, a good deal of data support the existence of chemokine receptor dimers (Springael et al., 2005), and for CXCR4, experiments suggest that ligand-induced conformational changes across the dimer may be important for receptor signaling (Percherancier et al., 2005).

E/D$^{3.49}$ (D126 in CXCR6) has been implicated in stabilizing both inactive and active receptor conformations (Jaakola et al., 2008; Scheerer et al., 2008), in the former case by interacting with the adjacent R$^{3.50}$. The canonical Y$^{3.51}$ has been identified as one of the 36 residues participating in the 24 inter-helical contacts that create the conserved structural scaffold for the class A GPCRs (Venkatakrishnan et al., 2013). Our molecular modeling identified some of the relevant interactions for the analogous residues in the CXCR6 structure, including between D126 (D$^{3.49}$) and the adjacent R127 and between F128 (F$^{3.51}$) and the residues C210 and V213 in helix five.

In dynamic modeling of the effects of the mutations in H3C of CXCR6, the F128Y and D126Y mutants, which showed loss of function in HEK-293T and Jurkat E6-1 cells, respectively, showed gross changes in the lengths and rotation angles of helix four, which were corrected toward wild-type values in the F128Y/V130A and D126Y/V130A double mutants. These structural corrections were associated with return to wild-type function in the cells where functional deficiencies had been evident. Models of F128Y and D126Y mutants also showed disruptions of a network of interactions including helix six (S229) and helix four (K143) via the D126–R127 salt bridge in helix three. This network was restored in the F128Y/V130A double mutant. It is of interest that although replacing V130 with A in CXCR6 had limited functional effect on its own, the compensatory effects of this substitution in the face of the D126Y or F128Y mutations were significant, both functionally and in the molecular modeling. Position 3.53 (V130 in CXCR6) is notable, since it has been shown to interact directly with G protein in activated structures of both rhodopsin (Deupi et al., 2012) and the β_2-adrenergic receptor (Rasmussen et al., 2011; Venkatakrishnan et al., 2013). Our modeling data are consistent with the size of the hydrophobic residue at this position being important for maintaining the local structure of the receptor in a way that, based on the known GPCR structures and our functional data, is likely to be important in binding G protein.

Molecular Pharmacology Fast Forward. Published on August 27, 2015 as DOI: 10.1124/mol.115.099960
This article has not been copyedited and formatted. The final version may differ from this version.

Because CXCR6 activity was fully inhibited by pertussis toxin, we investigated the pattern of use of $G_{i/o}$ proteins using an siRNA-based knockdown assay. Our data demonstrate that highly conserved residues within H3C are not only important for G protein binding per se, but also can determine selectivity among closely related G proteins. Published data on determinants of G protein selectivity among GPCRs rely primarily on chimeric receptors and involve changes in the use of G protein subfamilies, such as G_i vs. G_q (reviewed in (Wong, 2003) and (Moreira, 2014)). Most of the information available suggests that such selectivity is a function of the receptors' third intracellular loop, sometimes with contributions from residues in the second intracellular loop (Blin et al., 1995; Nasman et al., 1997; Ostrowski et al., 1992; Wong, 2003), although residues in helix six have also been implicated (Kostenis et al., 1997). Mutagenesis has identified the 3.53 position (V130 in CXCR6) in the m3 muscarinic acetylcholine receptor (C124) and the α_{2A}-adrenergic receptor (S134) in determining the specificity of coupling to G_i vs. G_q or G_i vs. G_s proteins, respectively (Blin et al., 1995; Nasman et al., 1997). Our data demonstrate that for the H3C region, subtle and cooperative changes can affect coupling to members of the $G_{i/o}$ subfamily selectively. As far as we are aware, there are no previous data implicating positions 3.49 or 3.51 in selectivity for coupling to G proteins generally, and although different receptor conformations have been shown to couple selectively to different members of the $G_{i/o}$ subfamily (Lane et al., 2007), we are not aware of any previous data that have addressed specific receptor residues important for selectivity among members of a single G protein subfamily.

It is notable that in our experiments knocking down $G\alpha_{□/o}$ subunits, non-wild-type function and CXCL16 binding correlated with a non-wild-type pattern of $G_{i/o}$ protein use, and a wild-type activity profile among the mutant receptors, including the normalized function of the CXCR6 F128Y/V130A and D126Y/V130A mutants in HEK-293T cells and Jurkat E6-1 cells, respectively, correlated more closely with a wild-type pattern of $G_{i/o}$ protein use. Overall, the knockdown data showed promiscuous use of the available $G_{i/o}$ proteins by the wild-type CXCR6, whereas the mutant proteins that displayed significantly compromised function showed selective defects in using one of the $G_{i/o}$ proteins. The data demonstrating

Molecular Pharmacology Fast Forward. Published on August 27, 2015 as DOI: 10.1124/mol.115.099960
This article has not been copyedited and formatted. The final version may differ from this version.

that CXCR6 depended on all the $G\alpha_{i/o}$ subunits suggested that a given $G_{i/o}$ protein cannot substitute for another, and is consistent with $G_{i/o}$ proteins being present, in toto, in limiting amounts. A surprising finding was that the sums of % inhibition in calcium flux assays resulting from knockdown of the various $G_{i/o}$ proteins exceeded 100, suggesting functional cooperation among $G\alpha_{i/o}$ subunits. We do not know an established mechanism that would explain this finding. One possibility might be allosteric effects of G protein binding to one protomer that would facilitate G protein binding to the second protomer in a receptor dimer.

It is of particular interest that the effects of the H3C mutations on downstream signaling were cell-type specific. Moreover, most clearly for the CXCR6 F128Y mutant, these cell-type specific effects could not be explained solely on the basis of intrinsic (cell-type independent) differences in the receptor's use of the various G proteins together with differences between the cell types in the abundances of $G\alpha_{i/o}$ subunits. As a hypothetical example of such a mechanism, a mutant showing an intrinsic (cell-type independent), skewed pattern of dependence on G_{i1} proteins might function well in HEK-293T cells, where the $G\alpha_{i1}$ subunit is expressed, but not in Jurkat E6-1 cells, where the $G\alpha_{i1}$ subunit is barely detectable. By contrast, for the F128Y mutant, we found a cell-type specific difference in the mutant protein's ability to use $G_{i/o}$ proteins. For that mutant, as compared with the wild-type receptor, the dependence on G_o proteins was compromised in HEK-293T cells, associated with diminished function, whereas in Jurkat E6-1 cells both the use of G_o proteins and receptor signaling were the same as wild-type. We are not aware of previous reports of such cell-type specific differences in the selective use of endogenous G proteins. We interpret these differences to be reflecting cell-type dependent receptor conformations. For the F128Y mutant, all the parameters that we measured were concordant, suggesting a non-wild-type conformation in HEK-293T cells and a wild-type conformation in Jurkat E6-1 cells. The factor(s) responsible for these cell-type specific differences in receptor conformations remain unknown.

Cell-type specific effects on GPCR activities have been well described (reviewed in (Kenakin and Miller, 2010)), including cell-type dependent differences in the abilities of receptors to use over-expressed

Molecular Pharmacology Fast Forward. Published on August 27, 2015 as DOI: 10.1124/mol.115.099960
This article has not been copyedited and formatted. The final version may differ from this version.

G proteins (Arai and Charo, 1996). Although the basis for cell-type specific differences has generally not been identified, variable levels of expression of regulators such as G-protein-coupled-receptor kinases (Tobin et al., 2008) has been suggested as one possible mechanism. Although receptor phosphorylation by G-protein-coupled-receptor kinases has not been shown to affect G protein binding and/or selectivity, phosphorylation by protein kinase A can induce β-adrenergic receptors to switch from G_s to G_i proteins (Daaka et al., 1997; Martin et al., 2004), suggesting that cell-type dependent phosphorylation and/or other covalent modifications of receptors could regulate receptor conformation and the specificity of receptor/G-protein coupling. Other categories of protein-protein interactions, such as GPCR:GPCR interactions, could also be cell-type specific and alter receptor conformations. In fact, heterodimerization of receptors has been shown to alter G protein selectivity (Breit et al., 2004).

Our observations provide a cautionary note in interpreting the significance of mutations in GPCRs when receptors are tested in a single system. More importantly, our findings suggest that the CXCR6 structure may have been optimized to perform in the range of cell types where the receptor is expressed by maintaining promiscuous use of $G_{i/o}$ proteins. It is worth noting in this regard that we have shown that even within closely related leukocyte populations, such as subsets of human T cells, there are significant differences in the $G_{i/o}$ protein repertoire (Foley et al., 2010). Our current data show that subtle changes in CXCR6 to match canonical sequences in the H3C can lead to cell-type specific deficiencies in the use of specific $G_{i/o}$ proteins, which can in turn compromise receptor function. A requirement for maintaining promiscuity in G protein coupling within multiple cellular environments may be an underappreciated determinant of the structure of chemokine receptors and other GPCRs.

Molecular Pharmacology Fast Forward. Published on August 27, 2015 as DOI: 10.1124/mol.115.099960
This article has not been copyedited and formatted. The final version may differ from this version.

Acknowledgments

We thank Ronald L. Rabin (FDA) for assistance with calcium flux assay, Owen Schwartz and Juraj Kabat of the Biological Imaging Facility (NIAID, NIH) for their assistance with confocal microscopy, Mike Tartakovsky and Stephan Bour (NIAID, NIH) for providing resources for the computational aspects of this project, and Reinhard Grisshammer and Wei Huang (NIDDK, NIH) for helpful discussions. This study utilized the high-performance computational capabilities of the Biowulf Linux cluster at the National Institutes of Health.

Authorship Contributions

Participated in research design: Singh, Farber

Conducted experiments: Singh, Foley, Zhang, Hurt, Richards

Contributed new reagents or analytical tools: Smith, Liao

Performed data analysis: Singh, Foley, Hurt, Farber

Wrote or contributed to the writing of the manuscript: Singh, Hurt, Farber

Molecular Pharmacology Fast Forward. Published on August 27, 2015 as DOI: 10.1124/mol.115.099960
This article has not been copyedited and formatted. The final version may differ from this version.

REFERENCES

Acharya S, Saad Y and Karnik SS (1997) Transducin-alpha C-terminal peptide binding site consists of C-D and E-F loops of rhodopsin. *J Biol Chem* **272**(10): 6519-6524.

Alkhatib G, Liao F, Berger EA, Farber JM and Peden KW (1997) A new SIV co-receptor, STRL33. *Nature* **388**(6639): 238.

Arai H and Charo IF (1996) Differential regulation of G-protein-mediated signaling by chemokine receptors. *J Biol Chem* **271**(36): 21814-21819.

Auger GA, Pease JE, Shen X, Xanthou G and Barker MD (2002) Alanine scanning mutagenesis of CCR3 reveals that the three intracellular loops are essential for functional receptor expression. *Eur J Immunol* **32**(4): 1052-1058.

Bachelerie F, Ben-Baruch A, Burkhardt AM, Combadiere C, Farber JM, Graham GJ, Horuk R, Sparre-Ulrich AH, Locati M, Luster AD, Mantovani A, Matsushima K, Murphy PM, Nibbs R, Nomiyama H, Power CA, Proudfoot AE, Rosenkilde MM, Rot A, Sozzani S, Thelen M, Yoshie O and Zlotnik A (2013) International Union of Pharmacology. LXXXIX. Update on the extended family of chemokine receptors and introducing a new nomenclature for atypical chemokine receptors. *Pharmacol Rev* **66**(1): 1-79.

Ballesteros J, Kitanovic S, Guarnieri F, Davies P, Fromme BJ, Konvicka K, Chi L, Millar RP, Davidson JS, Weinstein H and Sealfon SC (1998) Functional microdomains in G-protein-coupled receptors. The conserved arginine-cage motif in the gonadotropin-releasing hormone receptor. *J Biol Chem* **273**(17): 10445-10453.

Ballesteros JA, Jensen AD, Liapakis G, Rasmussen SG, Shi L, Gether U and Javitch JA (2001) Activation of the beta 2-adrenergic receptor involves disruption of an ionic lock between the cytoplasmic ends of transmembrane segments 3 and 6. *J Biol Chem* **276**(31): 29171-29177.

Ballesteros JA and Weinstein H (1995) Integrated methods for the construction of three-dimensional models and computational probing of structure-function relations in G protein coupled receptors. *Methods Neurosci* **25**: 366-428.

Blin N, Yun J and Wess J (1995) Mapping of single amino acid residues required for selective activation of Gq/11 by the m3 muscarinic acetylcholine receptor. *J Biol Chem* **270**(30): 17741-17748.

Breit A, Lagace M and Bouvier M (2004) Hetero-oligomerization between beta2- and beta3-adrenergic receptors generates a beta-adrenergic signaling unit with distinct functional properties. *J Biol Chem* **279**(27): 28756-28765.

Chen A, Gao ZG, Barak D, Liang BT and Jacobson KA (2001) Constitutive activation of A(3) adenosine receptors by site-directed mutagenesis. *Biochem Biophys Res Commun* **284**(3): 596-601.

Cherezov V, Rosenbaum DM, Hanson MA, Rasmussen SG, Thian FS, Kobilka TS, Choi HJ, Kuhn P, Weis WI, Kobilka BK and Stevens RC (2007) High-resolution crystal structure of an engineered human beta2-adrenergic G protein-coupled receptor. *Science* **318**(5854): 1258-1265.

Choe HW, Kim YJ, Park JH, Morizumi T, Pai EF, Krauss N, Hofmann KP, Scheerer P and Ernst OP (2011) Crystal structure of metarhodopsin II. *Nature* **471**(7340): 651-655.

Colvin RA, Campanella GS, Sun J and Luster AD (2004) Intracellular domains of CXCR3 that mediate CXCL9, CXCL10, and CXCL11 function. *J Biol Chem* **279**(29): 30219-30227.

Daaka Y, Luttrell LM and Lefkowitz RJ (1997) Switching of the coupling of the beta2-adrenergic receptor to different G proteins by protein kinase A. *Nature* **390**(6655): 88-91.

De Lean A, Stadel JM and Lefkowitz RJ (1980) A ternary complex model explains the agonist-specific binding properties of the adenylate cyclase-coupled beta-adrenergic receptor. *J Biol Chem* **255**(15): 7108-7117.

Deng HK, Unutmaz D, KewalRamani VN and Littman DR (1997) Expression cloning of new receptors used by simian and human immunodeficiency viruses. *Nature* **388**(6639): 296-300.

Deupi X, Edwards P, Singhal A, Nickle B, Oprian D, Schertler G and Standfuss J (2012) Stabilized G protein binding site in the structure of constitutively active metarhodopsin-II. *Proc Natl Acad Sci U S A* **109**(1): 119-124.

Doranz BJ, Orsini MJ, Turner JD, Hoffman TL, Berson JF, Hoxie JA, Peiper SC, Brass LF and Doms RW (1999) Identification of CXCR4 domains that support coreceptor and chemokine receptor functions. *J Virol* **73**(4): 2752-2761.

Foley JF, Singh SP, Cantu M, Chen L, Zhang HH and Farber JM (2010) Differentiation of human T cells alters their repertoire of G protein alpha-subunits. *J Biol Chem* **285**(46): 35537-35550.

Fraser CM, Wang CD, Robinson DA, Gocayne JD and Venter JC (1989) Site-directed mutagenesis of m1 muscarinic acetylcholine receptors: conserved aspartic acids play important roles in receptor function. *Mol Pharmacol* **36**(6): 840-847.

Frishman D and Argos P (1995) Knowledge-based protein secondary structure assignment. *Proteins* **23**(4): 566-579.

Hamm HE, Deretic D, Arendt A, Hargrave PA, Koenig B and Hofmann KP (1988) Site of G protein binding to rhodopsin mapped with synthetic peptides from the alpha subunit. *Science* **241**(4867): 832-835.

Hawtin SR (2005) Charged residues of the conserved DRY triplet of the vasopressin V1a receptor provide molecular determinants for cell surface delivery and internalization. *Mol Pharmacol* **68**(4): 1172-1182.

Hino T, Arakawa T, Iwanari H, Yurugi-Kobayashi T, Ikeda-Suno C, Nakada-Nakura Y, Kusano-Arai O, Weyand S, Shimamura T, Nomura N, Cameron AD, Kobayashi T, Hamakubo T, Iwata S and Murata T (2012) G-protein-coupled receptor inactivation by an allosteric inverse-agonist antibody. *Nature* **482**(7384): 237-240.

Humphrey W, Dalke A and Schulten K (1996) VMD: visual molecular dynamics. *J Mol Graph* **14**(1): 33-38, 27-38.

Huttenrauch F, Nitzki A, Lin FT, Honing S and Oppermann M (2002) Beta-arrestin binding to CC chemokine receptor 5 requires multiple C-terminal receptor phosphorylation sites and involves a conserved Asp-Arg-Tyr sequence motif. *J Biol Chem* **277**(34): 30769-30777.

Jaakola VP, Griffith MT, Hanson MA, Cherezov V, Chien EY, Lane JR, Ijzerman AP and Stevens RC (2008) The 2.6 angstrom crystal structure of a human A2A adenosine receptor bound to an antagonist. *Science* **322**(5905): 1211-1217.

Kenakin T and Miller LJ (2010) Seven transmembrane receptors as shapeshifting proteins: the impact of allosteric modulation and functional selectivity on new drug discovery. *Pharmacol Rev* **62**(2): 265-304.

Kiefer F, Arnold K, Kunzli M, Bordoli L and Schwede T (2009) The SWISS-MODEL Repository and associated resources. *Nucleic Acids Res* **37**(Database issue): 92.

Kim CH, Kunkel EJ, Boisvert J, Johnston B, Campbell JJ, Genovese MC, Greenberg HB and Butcher EC (2001) Bonzo/CXCR6 expression defines type 1-polarized T-cell subsets with extralymphoid tissue homing potential. *J Clin Invest* **107**(5): 595-601.

Kostenis E, Conklin BR and Wess J (1997) Molecular basis of receptor/G protein coupling selectivity studied by coexpression of wild type and mutant m2 muscarinic receptors with mutant G alpha(q) subunits. *Biochemistry* **36**(6): 1487-1495.

Lagane B, Ballet S, Planchenault T, Balabanian K, Le Poul E, Blanpain C, Percherancier Y, Staropoli I, Vassart G, Oppermann M, Parmentier M and Bachelerie F (2005) Mutation of the DRY motif reveals different structural requirements for the CC chemokine receptor 5-mediated signaling and receptor endocytosis. *Mol Pharmacol* **67**(6): 1966-1976.

Lane JR, Powney B, Wise A, Rees S and Milligan G (2007) Protean agonism at the dopamine D2 receptor: (S)-3-(3-hydroxyphenyl)-N-propylpiperidine is an agonist for activation of Go1 but an antagonist/inverse agonist for Gi1,Gi2, and Gi3. *Mol Pharmacol* **71**(5): 1349-1359.

Li J, Huang P, Chen C, de Riel JK, Weinstein H and Liu-Chen LY (2001) Constitutive activation of the mu opioid receptor by mutation of D3.49(164), but not D3.32(147): D3.49(164) is critical for stabilization of the inactive form of the receptor and for its expression. *Biochemistry* **40**(40): 12039-12050.

Liao F, Alkhatib G, Peden KW, Sharma G, Berger EA and Farber JM (1997) STRL33, A novel chemokine receptor-like protein, functions as a fusion cofactor for both macrophage-tropic and T cell line-tropic HIV-1. *J Exp Med* **185**(11): 2015-2023.

Liao F, Rabin RL, Smith CS, Sharma G, Nutman TB and Farber JM (1999) CC-chemokine receptor 6 is expressed on diverse memory subsets of T cells and determines responsiveness to macrophage inflammatory protein 3 alpha. *J Immunol* **162**(1): 186-194.

Liao F, Rabin RL, Yannelli JR, Koniaris LG, Vanguri P and Farber JM (1995) Human Mig chemokine: biochemical and functional characterization. *J Exp Med* **182**(5): 1301-1314.

Liao F, Shirakawa AK, Foley JF, Rabin RL and Farber JM (2002) Human B cells become highly responsive to macrophage-inflammatory protein-3 alpha/CC chemokine ligand-20 after cellular activation without changes in CCR6 expression or ligand binding. *J Immunol* **168**(10): 4871-4880.

Limou S, Coulonges C, Herbeck JT, van Manen D, An P, Le Clerc S, Delaneau O, Diop G, Taing L, Montes M, van't Wout AB, Gottlieb GS, Therwath A, Rouzioux C, Delfraissy JF, Lelievre JD, Levy Y, Hercberg S, Dina C, Phair J, Donfield S, Goedert JJ, Buchbinder S, Estaquier J, Schachter F, Gut I, Froguel P, Mullins JI, Schuitemaker H, Winkler C and Zagury JF (2010) Multiple-cohort genetic association study reveals CXCR6 as a new chemokine receptor involved in long-term nonprogression to AIDS. *J Infect Dis* **202**(6): 908-915.

Loetscher M, Amara A, Oberlin E, Brass N, Legler D, Loetscher P, D'Apuzzo M, Meese E, Rousset D, Virelizier JL, Baggiolini M, Arenzana-Seisdedos F and Moser B (1997) TYMSTR, a putative chemokine receptor selectively expressed in activated T cells, exhibits HIV-1 coreceptor function. *Curr Biol* **7**(9): 652-660.

Lu ZL, Curtis CA, Jones PG, Pavia J and Hulme EC (1997) The role of the aspartate-arginine-tyrosine triad in the m1 muscarinic receptor: mutations of aspartate 122 and tyrosine 124

decrease receptor expression but do not abolish signaling. *Mol Pharmacol* **51**(2): 234-241.

Martin NP, Whalen EJ, Zamah MA, Pierce KL and Lefkowitz RJ (2004) PKA-mediated phosphorylation of the beta1-adrenergic receptor promotes Gs/Gi switching. *Cell Signal* **16**(12): 1397-1403.

Matloubian M, David A, Engel S, Ryan JE and Cyster JG (2000) A transmembrane CXC chemokine is a ligand for HIV-coreceptor Bonzo. *Nat Immunol* **1**(4): 298-304.

Mezei M (2010) Simulaid: a simulation facilitator and analysis program. *J Comput Chem* **31**(14): 2658-2668.

Moreira IS (2014) Structural features of the G-protein/GPCR interactions. *Biochim Biophys Acta* **1840**(1): 16-33.

Nasman J, Jansson CC and Akerman KE (1997) The second intracellular loop of the alpha2-adrenergic receptors determines subtype-specific coupling to cAMP production. *J Biol Chem* **272**(15): 9703-9708.

Ostrowski J, Kjelsberg MA, Caron MG and Lefkowitz RJ (1992) Mutagenesis of the beta 2-adrenergic receptor: how structure elucidates function. *Annu Rev Pharmacol Toxicol* **32**: 167-183.

Percherancier Y, Berchiche YA, Slight I, Volkmer-Engert R, Tamamura H, Fujii N, Bouvier M and Heveker N (2005) Bioluminescence resonance energy transfer reveals ligand-induced conformational changes in CXCR4 homo- and heterodimers. *J Biol Chem* **280**(11): 9895-9903.

Phillips JC, Braun R, Wang W, Gumbart J, Tajkhorshid E, Villa E, Chipot C, Skeel RD, Kale L and Schulten K (2005) Scalable molecular dynamics with NAMD. *J Comput Chem* **26**(16): 1781-1802.

Prado GN, Taylor L and Polgar P (1997) Effects of intracellular tyrosine residue mutation and carboxyl terminus truncation on signal transduction and internalization of the rat bradykinin B2 receptor. *J Biol Chem* **272**(23): 14638-14642.

Rabin RL, Park MK, Liao F, Swofford R, Stephany D and Farber JM (1999) Chemokine receptor responses on T cells are achieved through regulation of both receptor expression and signaling. *J Immunol* **162**(7): 3840-3850.

Rasmussen SG, DeVree BT, Zou Y, Kruse AC, Chung KY, Kobilka TS, Thian FS, Chae PS, Pardon E, Calinski D, Mathiesen JM, Shah ST, Lyons JA, Caffrey M, Gellman SH, Steyaert J, Skiniotis G, Weis WI, Sunahara RK and Kobilka BK (2011) Crystal structure of the beta2 adrenergic receptor-Gs protein complex. *Nature* **477**(7366): 549-555.

Rasmussen SG, Jensen AD, Liapakis G, Ghanouni P, Javitch JA and Gether U (1999) Mutation of a highly conserved aspartic acid in the beta2 adrenergic receptor: constitutive activation, structural instability, and conformational rearrangement of transmembrane segment 6. *Mol Pharmacol* **56**(1): 175-184.

Roland J, Murphy BJ, Ahr B, Robert-Hebmann V, Delauzun V, Nye KE, Devaux C and Biard-Piechaczyk M (2003) Role of the intracellular domains of CXCR4 in SDF-1-mediated signaling. *Blood* **101**(2): 399-406.

Rosenbaum DM, Cherezov V, Hanson MA, Rasmussen SG, Thian FS, Kobilka TS, Choi HJ, Yao XJ, Weis WI, Stevens RC and Kobilka BK (2007) GPCR engineering yields high-

resolution structural insights into beta2-adrenergic receptor function. *Science* **318**(5854): 1266-1273.

Rovati GE, Capra V and Neubig RR (2007) The highly conserved DRY motif of class A G protein-coupled receptors: beyond the ground state. *Mol Pharmacol* **71**(4): 959-964.

Satoh-Takayama N, Serafini N, Verrier T, Rekiki A, Renauld JC, Frankel G and Di Santo JP (2014) The chemokine receptor CXCR6 controls the functional topography of interleukin-22 producing intestinal innate lymphoid cells. *Immunity* **41**(5): 776-788.

Scheer A, Fanelli F, Costa T, De Benedetti PG and Cotecchia S (1997) The activation process of the alpha1B-adrenergic receptor: potential role of protonation and hydrophobicity of a highly conserved aspartate. *Proc Natl Acad Sci U S A* **94**(3): 808-813.

Scheerer P, Park JH, Hildebrand PW, Kim YJ, Krauss N, Choe HW, Hofmann KP and Ernst OP (2008) Crystal structure of opsin in its G-protein-interacting conformation. *Nature* **455**(7212): 497-502.

Springael JY, Urizar E and Parmentier M (2005) Dimerization of chemokine receptors and its functional consequences. *Cytokine Growth Factor Rev* **16**(6): 611-623.

Standfuss J, Edwards PC, D'Antona A, Fransen M, Xie G, Oprian DD and Schertler GF (2011) The structural basis of agonist-induced activation in constitutively active rhodopsin. *Nature* **471**(7340): 656-660.

Tobin AB, Butcher AJ and Kong KC (2008) Location, location, location...site-specific GPCR phosphorylation offers a mechanism for cell-type-specific signalling. *Trends Pharmacol Sci* **29**(8): 413-420.

Venkatakrishnan AJ, Deupi X, Lebon G, Tate CG, Schertler GF and Babu MM (2013) Molecular signatures of G-protein-coupled receptors. *Nature* **494**(7436): 185-194.

Warne T, Serrano-Vega MJ, Baker JG, Moukhametzianov R, Edwards PC, Henderson R, Leslie AG, Tate CG and Schertler GF (2008) Structure of a beta1-adrenergic G-protein-coupled receptor. *Nature* **454**(7203): 486-491.

Whorton MR, Bokoch MP, Rasmussen SG, Huang B, Zare RN, Kobilka B and Sunahara RK (2007) A monomeric G protein-coupled receptor isolated in a high-density lipoprotein particle efficiently activates its G protein. *Proc Natl Acad Sci U S A* **104**(18): 7682-7687.

Wilbanks A, Zondlo SC, Murphy K, Mak S, Soler D, Langdon P, Andrew DP, Wu L and Briskin M (2001) Expression cloning of the STRL33/BONZO/TYMSTRligand reveals elements of CC, CXC, and CX3C chemokines. *J Immunol* **166**(8): 5145-5154.

Wong SK (2003) G protein selectivity is regulated by multiple intracellular regions of GPCRs. *Neurosignals* **12**(1): 1-12.

Wu B, Chien EY, Mol CD, Fenalti G, Liu W, Katritch V, Abagyan R, Brooun A, Wells P, Bi FC, Hamel DJ, Kuhn P, Handel TM, Cherezov V and Stevens RC (2010) Structures of the CXCR4 chemokine GPCR with small-molecule and cyclic peptide antagonists. *Science* **330**(6007): 1066-1071.

Wu D, Huang CK and Jiang H (2000) Roles of phospholipid signaling in chemoattractant-induced responses. *J Cell Sci* **113 (Pt 17)**: 2935-2940.

Zhang YJ, Zhang L, Ketas T, Korber BT and Moore JP (2001) HIV type 1 molecular clones able to use the Bonzo/STRL-33 coreceptor for virus entry. *AIDS Res Hum Retroviruses* **17**(3): 217-227.

Zhu SZ, Wang SZ, Hu J and el-Fakahany EE (1994) An arginine residue conserved in most G protein-coupled receptors is essential for the function of the m1 muscarinic receptor. *Mol Pharmacol* **45**(3): 517-523.

Molecular Pharmacology Fast Forward. Published on August 27, 2015 as DOI: 10.1124/mol.115.099960
This article has not been copyedited and formatted. The final version may differ from this version.

Footnote

This research was supported by the Intramural Research Program of the National Institute of Allergy and Infectious Diseases, National Institutes of Health.

Molecular Pharmacology Fast Forward. Published on August 27, 2015 as DOI: 10.1124/mol.115.099960
This article has not been copyedited and formatted. The final version may differ from this version.

Figure Legends

Fig. 1. The sequence of CXCR6 has atypical features. (A) Schematic representation of the wild-type CXCR6 receptor. The cell membrane is represented by the blue band. Amino acids in transmembrane alpha helices are shown in stacked triplets. CXCR6 contains residues, shown in light blue, that are conserved in GPCRs, such as N-linked glycosylation site(s) in the amino-terminal domain (N16 with branched structure), cysteines in extracellular loops one and two (C102 and C180), as well as sequences that are characteristic of chemokine receptors, such as paired acidic residues in the amino-terminal domain (E8 and D9, E21 and E22), a paired cysteine and tyrosine (C210 and Y211) and a cysteine in TMD VII (C282). Residues that we changed by site-directed mutagenesis are indicated in green with red letters. (B) Amino acid sequence alignment of H3C in CXCR6 and other chemokine receptors. Residue numbers 3.46 and 3.55 are according to the convention of Ballesteros and Weinstein (Ballesteros and Weinstein, 1995) (see text). (C) Sequences of CXCR6 wild-type and mutants that we produced and studied. Numbers designate CXCR6 I123 and V131. Canonical residues are red and non-canonical residues are blue. (D) Sequences of CCR6 wild-type and mutants that we produced and studied. Numbers designate CCR6 I139 and I147. Canonical residues are red and non-canonical residues are blue.

Fig. 2. Replacing D126 with Y leads to redistribution of CXCR6 in HEK-293T cells. Cells were transfected with equal amounts of pcDNA3.1, pEYFP-N1 and DNAs encoding CXCR6-YFP wild-type and mutant receptors. Cells transfected with pcDNA3.1 were incubated with a PE-conjugated isotype control antibody and other cells were incubated with anti-human CXCR6-PE. (A) Histograms showing YFP expression for pcDNA3.1 transfected cells in the shaded and cells transfected with pEYFP-N1 or CXCR6 DNAs in non-shaded histograms outlined in blue. Mean fluorescent intensities (MFIs) of YFP expressing cells are shown. Data are from one of more than five experiments. (B) Histograms showing CXCR6 surface staining in duplicate panels for the same cells as in (A). Data are from one of more than five experiments. (C) Confocal microscopy of cells transfected with pcDNA3.1 or DNAs encoding CXCR6-YFP wild-type and mutant receptors. The nuclei were stained with Hoechst 33342, shown in blue,

Molecular Pharmacology Fast Forward. Published on August 27, 2015 as DOI: 10.1124/mol.115.099960
This article has not been copyedited and formatted. The final version may differ from this version.

and emission from the YFP fusion proteins is shown in yellow. Data are from one of more than five experiments.

Fig. 3. CXCR6-F128Y has impaired activity when expressed in HEK-293T cells. (A) Cells were transfected with equal amounts of DNA encoding wild-type and mutant CXCR6-YFP proteins. Migration was measured using a microchemotaxis chamber with polycarbonate membranes and containing CXCL16 in the lower wells as described in Materials and Methods. The left panel shows means ± SEM of data from four experiments. The asterisks indicate a significant difference from HEK-293T cells expressing wild-type receptor and, as indicated by the bar, between CXCR6-F128Y and CXCR6-F128Y/V130A mutants. The right panel shows means ± SEM for chemotaxis using various concentrations of CXCL16 from three experiments using cells expressing wild-type or CXCR6-F128Y receptors. (B) Cells transfected as in (A) were fixed and stained with Alexa Fluor 488 phalloidin-paraformaldehyde at the indicated time points after stimulation with 2.5 μg/ml CXCL16 as described in Materials and Methods. All results are plotted relative to the mean fluorescence intensity (MFI) of the sample without the addition of CXCL16, which was set at 100% and plotted at 0 s. Data shown are from one of three experiments. Mean responses at each time point were calculated from the three experiments, and the asterisks indicate significant differences between the curves for F128Y vs. wild-type receptors and, as indicated by the bar, for mutants F128Y vs. F128Y/V130A. (C) Cells were transfected with variable amounts of DNAs encoding wild-type and mutant CXCR6-YFP proteins in order to produce equal surface expression. In the experiment shown in the left panel, cells were loaded with Fura-2/AM and assayed for intracellular calcium mobilization on a spectrofluorometer in response to 1 μg/ml CXCL16 added at the times indicated by the arrows as described in Materials and Methods. The numbers in each panel show peak changes in fluorescence ratios. This experiment is representative of four. Mean peak responses were calculated from the four experiments and the asterisks indicate significant differences between F128Y vs. wild-type receptors and, as indicated by the bar, mutants F128Y vs. F128Y/V130A (right panel). *, $P < 0.05$; **, $P < 0.01$; ***, $P < 0.001$.

Molecular Pharmacology Fast Forward. Published on August 27, 2015 as DOI: 10.1124/mol.115.099960
This article has not been copyedited and formatted. The final version may differ from this version.

Fig. 4. CXCR6-D126Y has impaired activity when expressed in Jurkat E6-1 cells. (A) Cells were transfected with variable amounts of DNAs encoding wild-type and mutant CXCR6-YFP receptors, in order to produce equal surface expression. In each experiment, the means were obtained for the % of input cells migrating to duplicate wells of a Transwell plate as described in Materials and Methods. The left panel shows means ± SEM of data from three experiments. The asterisks indicate a significant difference from Jurkat E6-1 cells expressing wild-type receptor or between the groups connected by the horizontal bars. The right panel shows means ± SEM of data from three experiments using cells transfected with wild-type CXCR6 DNA or CXCR6-D126Y DNA and lower wells containing various concentrations of CXCL16. (B) Cells transfected with equal amounts of DNA encoding wild-type and mutant CXCR6-YFP proteins were fixed and stained with Alexa Fluor 488 phalloidin-paraformaldehyde at the indicated times after stimulation with 2.5 μg/ml CXCL16 as described in Materials and Methods. All results are plotted relative to the MFI of the cells without the addition of CXCL16 which was set at 100% and plotted at 0 s. Mean responses at each time point were calculated from the three experiments, and the asterisks indicate significant differences between the curves for D126Y vs. wild-type receptors. (C) Cells transfected as in (A) were loaded with Fura-2/AM and assayed for intracellular calcium mobilization on a spectrofluorometer in response to 1 μg/ml CXCL16 as described in Materials and Methods. Mean peak responses ± SEM were calculated from five experiments and the asterisks indicate significant differences between D126Y vs. wild-type receptors and, as indicated by the bar, mutants D126Y vs. D126Y/V130A. *, $P < 0.05$; **, $P < 0.01$; ***, $P < 0.001$.

Fig. 5. Molecular models of CXCR6. (A) C-alpha RMSDs are shown versus simulation time. (B**)** Median length of helix four is shown for WT and mutant receptors**.** Boxes depict upper and lower inner quartiles. Whiskers indicate maximum and minimum values. (C) Median rotation of helix four is shown for WT and mutant receptors**.** Boxes depict upper and lower inner quartiles. Whiskers indicate maximum and minimum values. (D**)** Abstract networks diagram of molecular interactions are shown for CXCR6 wild-type and mutant receptors. An orange diagonal line separates the protomers. Hydrogen bonds are red,

Molecular Pharmacology Fast Forward. Published on August 27, 2015 as DOI: 10.1124/mol.115.099960
This article has not been copyedited and formatted. The final version may differ from this version.

neighboring interactions are green. The width of the line connecting the nodes is proportional to the frequency with which the interaction is observed in the MD simulation (analogous to the strength of the interaction). Dark red and green lines indicate significant ($P < 0.001$) deviation in frequency from the wild type, either increased or decreased as reflected in the lines' widths. Mutant residues are shown as blue nodes. Arrows indicate patterns of variation. Jagged ellipses indicate fraying of helix four from (B). Curved arrows show rotation of helix four from (C). (E**)** Illustration of helix four shortening is shown for CXCR6 wild-type and mutant receptors using averaged structures. The ribbon figures overlay "averaged" structures from each simulation. Lipid and solvent molecules are not shown for clarity. Some helices are omitted and a single protomer is shown for clarity. Wild-type CXCR6 is blue, CXCR6-D126Y mutant is red, and CXCR6-D126Y/V130A mutant is green. Dotted lines indicate hydrogen bonds. (F) Illustration of helix four rotation is shown for CXCR6 wild-type and mutant receptors using averaged structures. The ribbon figures overlay "averaged" structures from each simulation. Some helices are omitted and no lipid or solvent molecules are shown for clarity. Wild-type CXCR6 is blue, CXCR6-V130A mutant is yellow, CXCR6-F128Y mutant is orange, and CXCR6-F128Y/V130 mutant is purple. Dotted lines indicate hydrogen bonds. Solid black lines separate protomers. The asterisks in (B) and (C) indicate a significant difference from wild-type or between the groups connected by the horizontal bars. **, $P < 0.01$; ****, $P < 0.0001$.

Fig. 6. Selective use of $G_{i/o}$ proteins by CXCR6 mutants in HEK-293T cells. (A) Cells co-transfected with equal amounts of CXCR6-WT or mutant plasmids and indicated siRNAs were harvested 72 hours later, loaded with Fura-2/AM, and assayed for intracellular calcium mobilization on a spectrofluorometer in response to 1 μg/ml CXCL16 as described in Materials and Methods. Using cells expressing each receptor, percent inhibition of peak ratio fluorescence by siRNAs knocking down individual Gα proteins as compared with cells transfected with control siRNAs were calculated. Shown are means ± SEM from three independent experiments. The asterisks indicate a significant difference from cells expressing wild-type receptor. *, $P < 0.05$; **, $P < 0.01$; ***, $P < 0.001$.

Molecular Pharmacology Fast Forward. Published on August 27, 2015 as DOI: 10.1124/mol.115.099960
This article has not been copyedited and formatted. The final version may differ from this version.

Fig. 7. Selective use of $G_{i/o}$ proteins by CXCR6 mutants in Jurkat E6-1 cells**.** Cells co-transfected with equal amounts of CXCR6-WT or mutant plasmids and indicated siRNAs were harvested 72 hours later, loaded with Fura-2/AM, and assayed for intracellular calcium mobilization on a spectrofluorometer in response to 1 μg/ml CXCL16 as described in Materials and Methods. Using cells expressing each receptor, percent inhibition of peak ratio fluorescence by siRNAs knocking down individual Gα proteins as compared with cells transfected with control siRNAs were calculated. Shown are means ± SEM from three independent experiments. The asterisks indicate a significant difference from cells expressing wild-type receptor. *, $P < 0.05$; **, $P < 0.01$; ***, $P < 0.001$.

Fig. 8. Changing canonical to non-canonical amino acids diminishes CCR6 activity in HEK-293T and Jurkat E6-1 cells. **(**A) HEK-293T cells were transfected with variable amounts of DNAs encoding wild-type and mutant CCR6-YFP receptors, in order to produce equal surface expression. Migration was measured using a microchemotaxis chamber containing CCL20 in the lower wells as described in Materials and Methods. Data shown are means ± SEM from four experiments. The asterisks indicate a significant difference from HEK-293T cells expressing wild-type receptor and as indicated by the bar, between cells expressing CCR6-D142Y and CCR6-D142Y/A146V. (B) Cells transfected as in (A), were loaded with Fura-2/AM and assayed for intracellular calcium mobilization on a spectrofluorometer in response to 1 μg/ml CCL20 as described in Materials and Methods. Data shown are mean ± SEM of three experiments. The asterisks indicate a significant difference from cells expressing wild-type receptor and as indicated by the bar, between cells expressing CCR6-D142Y and CCR6-D142Y/A146V. (C) Jurkat E6-1 cells were transfected with variable amounts of DNAs encoding wild-type and mutant CCR6-YFP receptors, in order to produce equal surface expression. In each experiment, the means were obtained for the % of input cells migrating to duplicate lower wells of a Transwell plate as described in Materials and Methods. Data shown are means ± SEM from three experiments. The asterisks indicate a significant difference from Jurkat E6-1 cells expressing wild-type receptor or between the cells connected by the horizontal bars. (D) Cells transfected as in (C), were loaded with Fura-2/AM and assayed for intracellular

Molecular Pharmacology Fast Forward. Published on August 27, 2015 as DOI: 10.1124/mol.115.099960
This article has not been copyedited and formatted. The final version may differ from this version.

calcium mobilization on a spectrofluorometer in response to 1 μg/ml CCL20 as described in Materials and Methods. Data shown are mean ± SEM of three experiments. The asterisks indicate a significant difference from cells expressing wild-type receptor or as indicated by the bar, between cells expressing CCR6-D142Y and CCR6-D142Y/A146V. *, $P < 0.05$; **, $P < 0.01$; ***, $P < 0.001$.

Molecular Pharmacology Fast Forward. Published on August 27, 2015 as DOI: 10.1124/mol.115.099960
This article has not been copyedited and formatted. The final version may differ from this version.

Table 1: S**ummary of the functional properties of CXCR6-WT and mutant receptors.**

HEK-293T cells

Receptor	Surface expression [a,b]	K_d [a,c]	Chemotaxis [a,b]	Calcium flux [a,b,d]	Actin polymerization [a,b]
CXCR6-WT	100	100	100	100	100
CXCR6-D126Y	37**	54***	96	102	93
CXCR6-F128Y	107	201***	42***	69**	68**
CXCR6-V130A	114	99	75**	93	77
CXCR6-D126Y/V130A	33**	56***	92	111	80
CXCR6-F128Y/V130A	110	96	78	104	80

Jurkat E6-1 cells

Receptor	Surface expression [a,b]	K_d [a,c]	Chemotaxis [a,b,d]	Calcium flux [a,b,d]	Actin polymerization [a,b]
CXCR6-WT	100	100	100	100	100
CXCR6-D126Y	51**	40**	35***	71**	71**
CXCR6-F128Y	98	75	83	103	94
CXCR6-V130A	125	96	75	96	96
CXCR6-D126Y/V130A	61**	35**	67*	92	95
CXCR6-F128Y/V130A	103	117	95	100	95

[a] All the values are means of the data from at least three experiments, normalized to values for the wild-type receptor, which were set to 100.
[b] Numbers <100 indicate less expression or activity compared to wild-type.
[c] K*d*'s <100 or >100 indicate higher or lower affinity, respectively, compared to wild-type.
[d] Cells were transfected with variable amounts of DNAs encoding wild-type and mutant CXCR6-YFP receptors in order to produce equal surface expression.
*, $P < 0.05$; **, $P < 0.01$; ***, $P < 0.001$ compared to the wild-type receptor based on the primary experimental data.

Molecular Pharmacology Fast Forward. Published on August 27, 2015 as DOI: 10.1124/mol.115.099960
This article has not been copyedited and formatted. The final version may differ from this version.

A

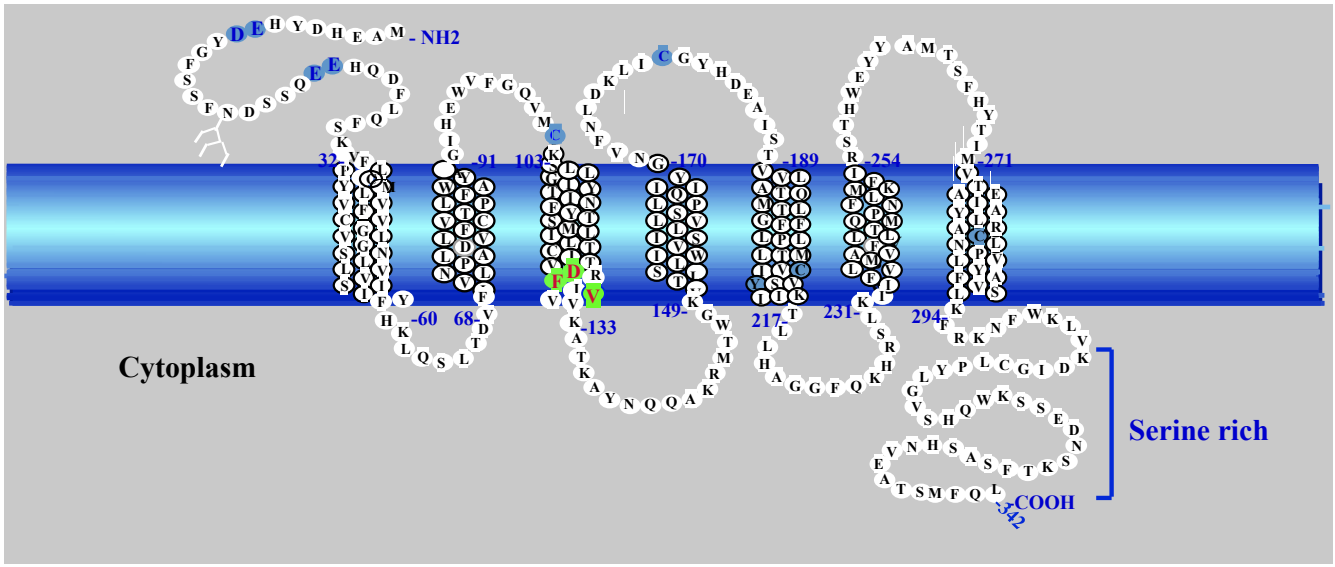

B

	3.46							3.55
CCR1	L	T	I	D	R	Y	L	A	I	V
CCR2	L	T	I	D	R	Y	L	A	I	V
CCR3	L	T	I	D	R	Y	L	A	I	V
CCR4	M	S	I	D	R	Y	L	A	I	V
CCR5	L	T	I	D	R	Y	L	A	V	V
CCR6	I	S	M	D	R	Y	I	A	I	V
CCR7	I	S	I	D	R	Y	V	A	I	V
CCR8	M	S	V	D	R	Y	L	A	V	V
CCR9	I	S	V	D	R	Y	I	A	I	A
CCR10	I	S	A	D	R	Y	V	A	I	A
CXCR1	I	S	V	D	R	Y	L	A	I	V
CXCR2	I	S	V	D	R	Y	L	A	I	V
CXCR3	I	S	F	D	R	Y	L	N	I	V
CXCR4	I	S	L	D	R	Y	L	A	I	V
CXCR5	I	A	V	D	R	Y	L	A	I	V
CXCR6	I	T	V	D	R	F	I	V	V	V
CXCR7	M	S	V	D	R	Y	L	S	I	T
CXCR8	I	A	V	D	R	Y	V	A	V	R
CX3CR1	I	S	I	D	R	Y	L	A	I	V
XCR1	M	T	I	H	R	Y	L	S	V	V

C

Amino acid position	123							131
Canonical sequence	I	T	V	D	R	Y	I	A	V
CXCR6-WT	I	T	V	D	R	F	I	V	V
CXCR6-D126Y	I	T	V	Y	R	F	I	V	V
CXCR6-F128Y	I	T	V	D	R	Y	I	V	V
CXCR6-V130A	I	T	V	D	R	F	I	A	V
CXCR6-D126Y/V130A	I	T	V	Y	R	F	I	A	V
CXCR6-F128Y/V130A	I	T	V	D	R	Y	I	A	V

D

Amino acid position	139							147
Canonical sequence	I	S	M	D	R	Y	I	A	I
CCR6-WT	I	S	M	D	R	Y	I	A	I
CCR6-D142Y	I	S	M	Y	R	Y	I	A	I
CCR6-Y144F	I	S	M	D	R	F	I	A	I
CCR6-A146V	I	S	M	D	R	Y	I	V	I
CCR6-D142Y/A146V	I	S	M	Y	R	Y	I	V	I
CCR6-Y144F/A146V	I	S	M	D	R	F	I	V	I

Figure 1

Molecular Pharmacology Fast Forward. Published on August 27, 2015 as DOI: 10.1124/mol.115.099960
This article has not been copyedited and formatted. The final version may differ from this version.

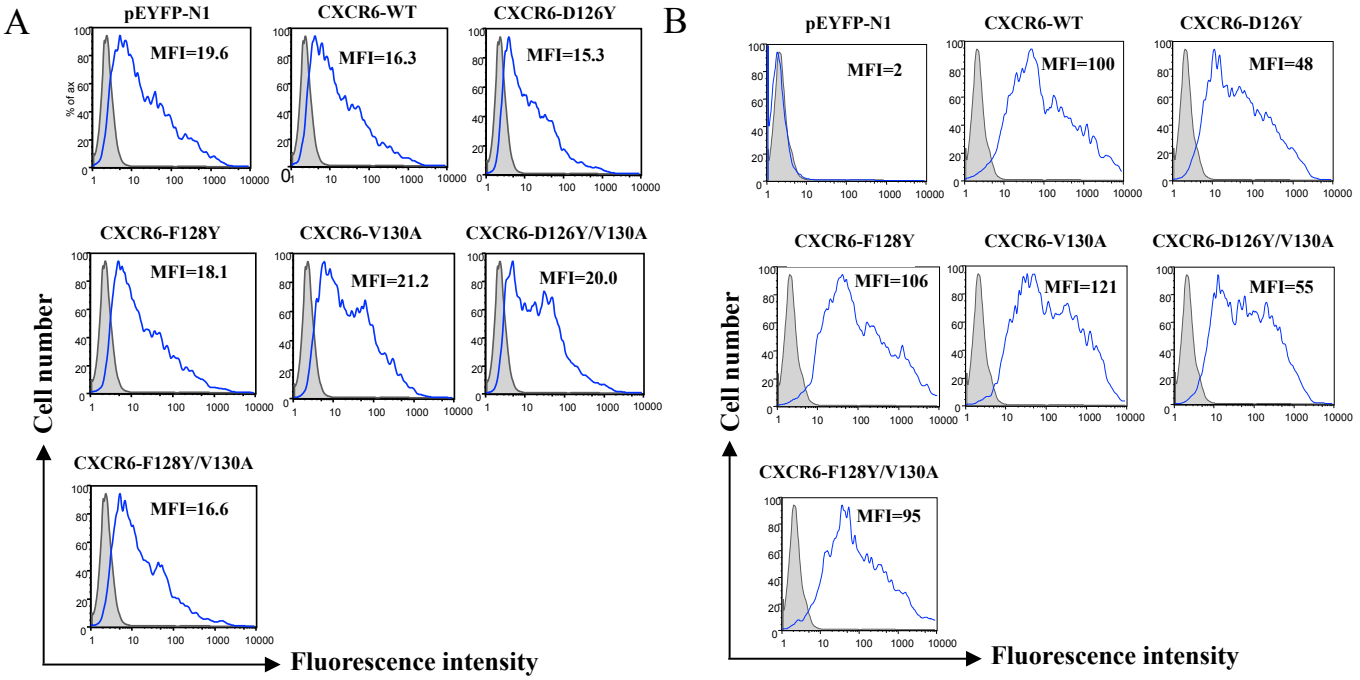

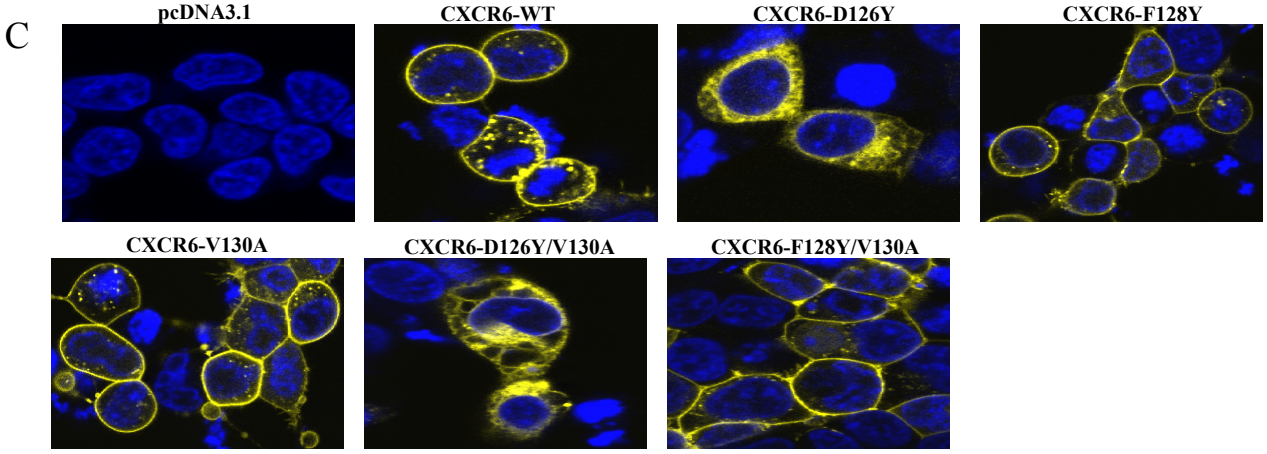

Figure 2

Molecular Pharmacology Fast Forward. Published on August 27, 2015 as DOI: 10.1124/mol.115.099960
This article has not been copyedited and formatted. The final version may differ from this version.

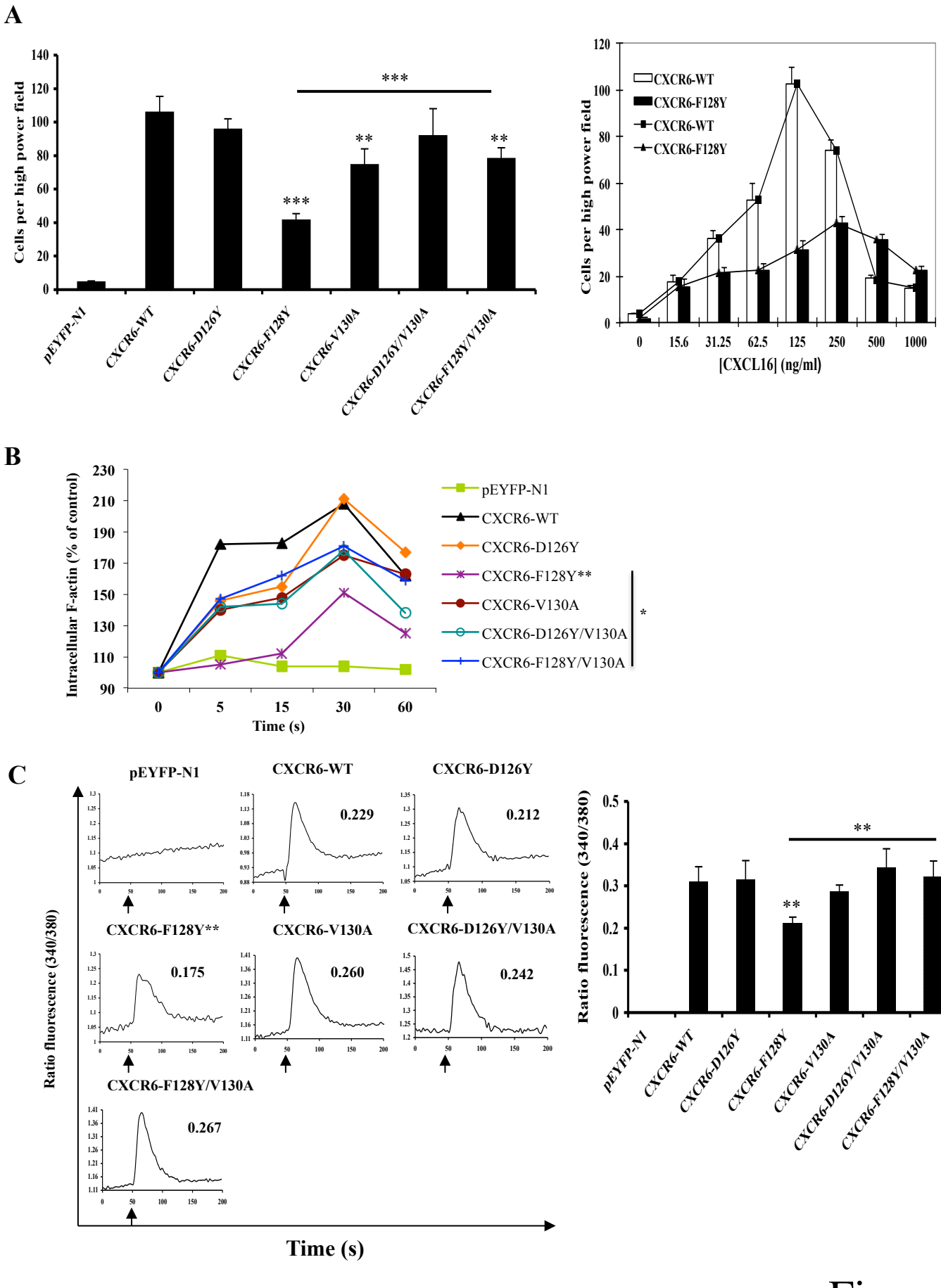

Figure 3

Molecular Pharmacology Fast Forward. Published on August 27, 2015 as DOI: 10.1124/mol.115.099960
This article has not been copyedited and formatted. The final version may differ from this version.

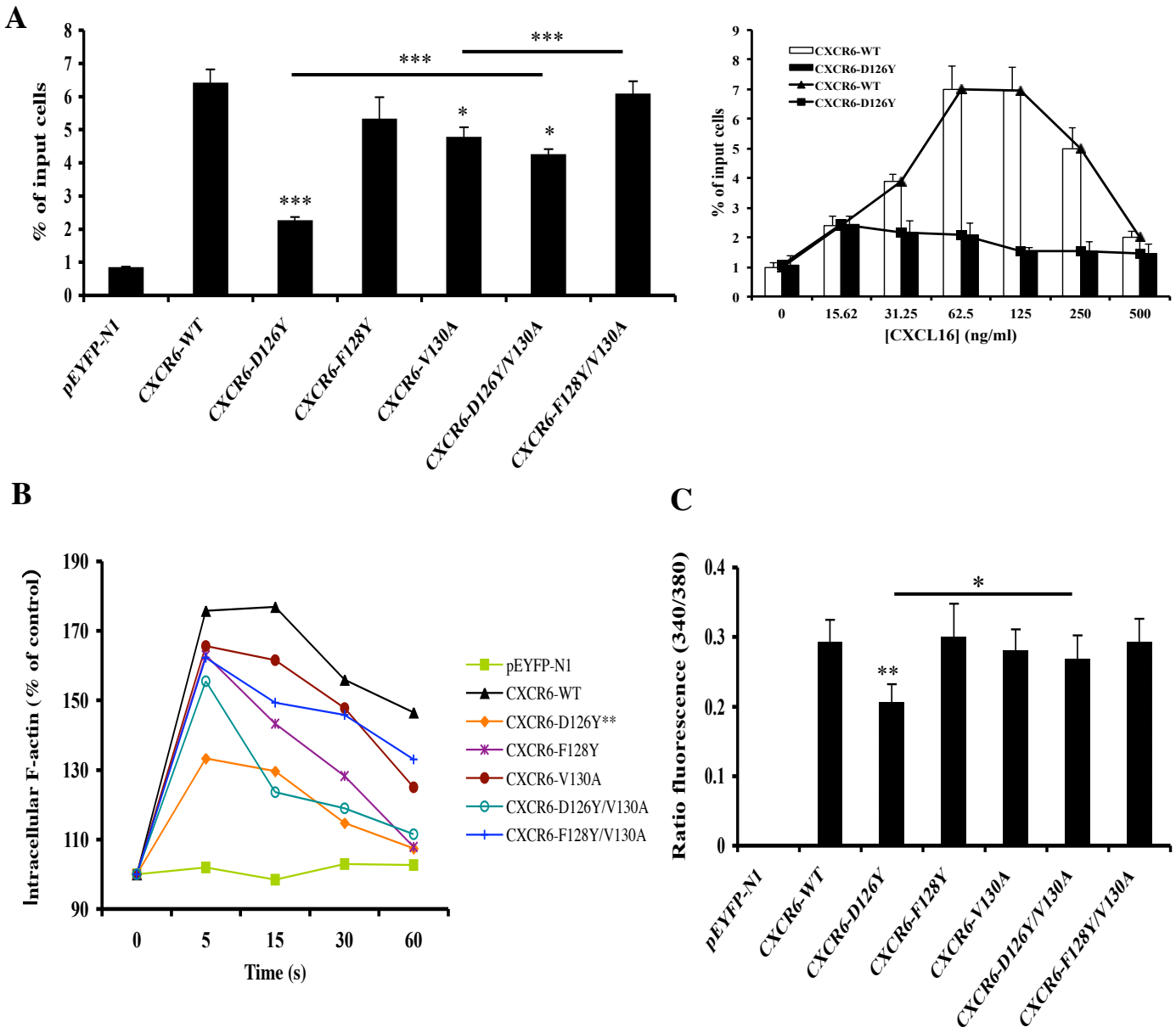

Figure 4

Molecular Pharmacology Fast Forward. Published on August 27, 2015 as DOI: 10.1124/mol.115.099960
This article has not been copyedited and formatted. The final version may differ from this version.

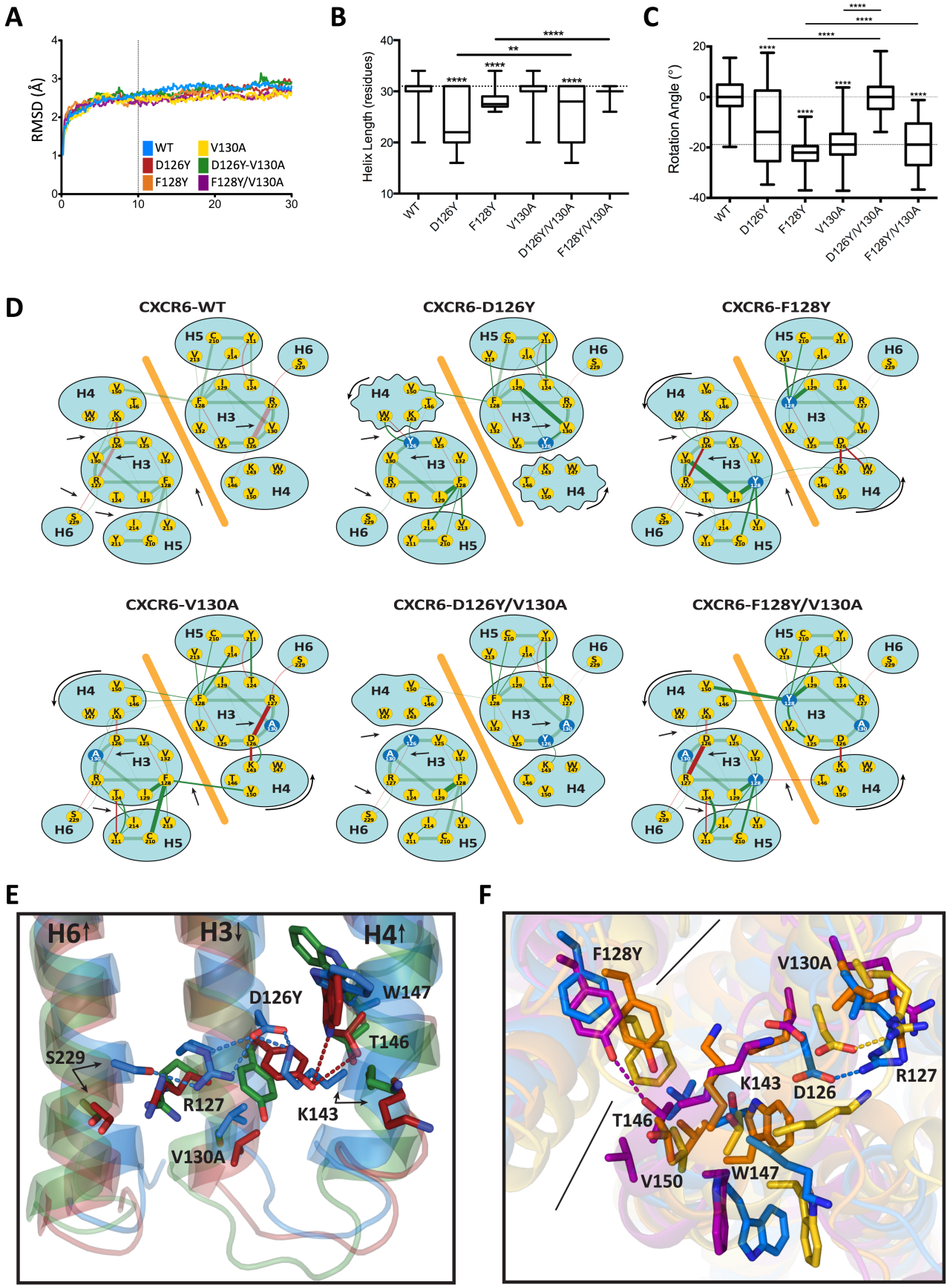

Figure 5

Molecular Pharmacology Fast Forward. Published on August 27, 2015 as DOI: 10.1124/mol.115.099960
This article has not been copyedited and formatted. The final version may differ from this version.

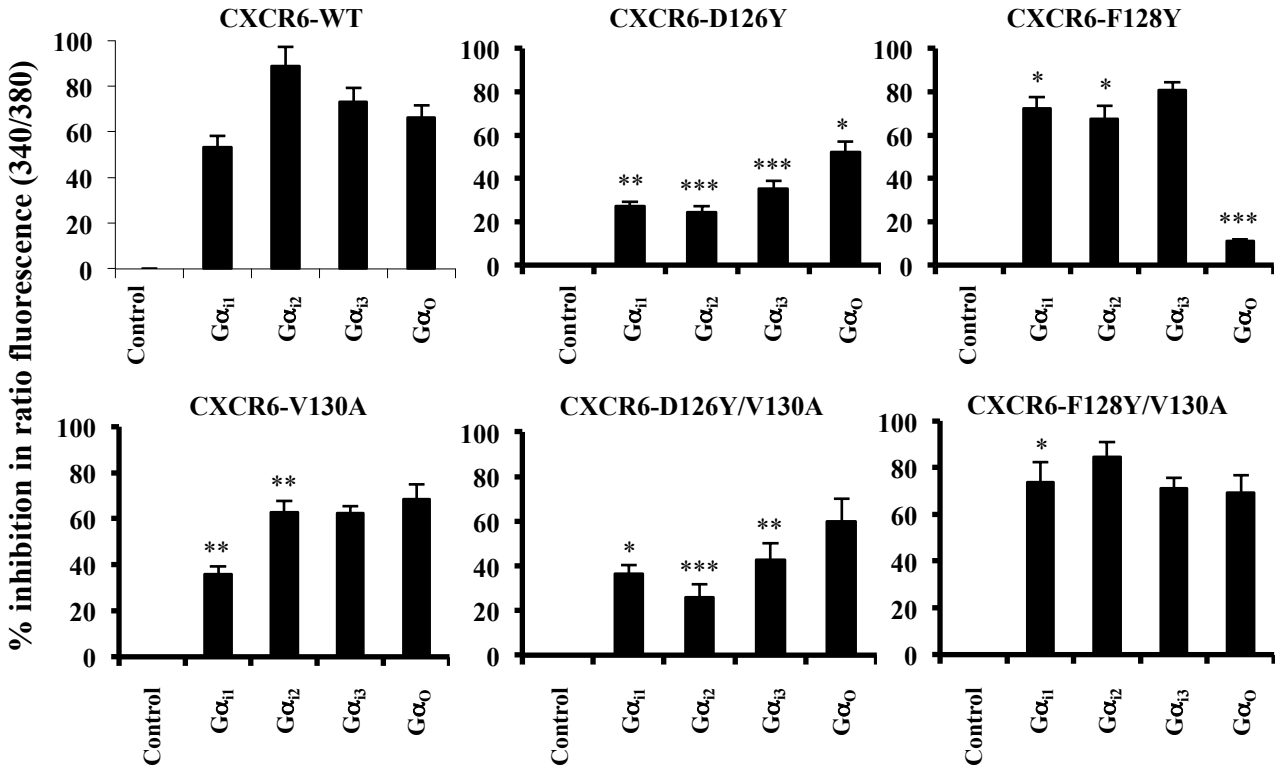

Figure 6

Molecular Pharmacology Fast Forward. Published on August 27, 2015 as DOI: 10.1124/mol.115.099960
This article has not been copyedited and formatted. The final version may differ from this version.

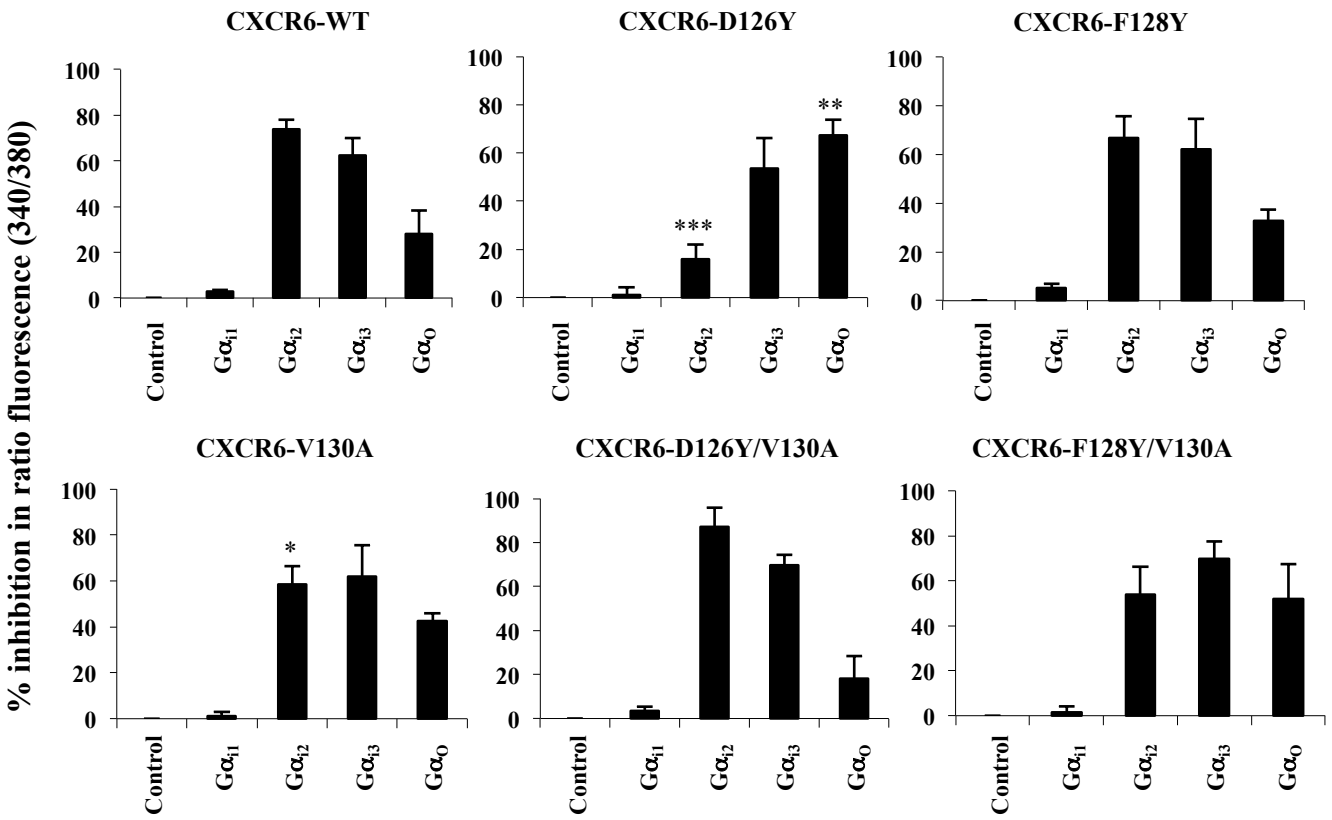

Figure 7

Molecular Pharmacology Fast Forward. Published on August 27, 2015 as DOI: 10.1124/mol.115.099960
This article has not been copyedited and formatted. The final version may differ from this version.

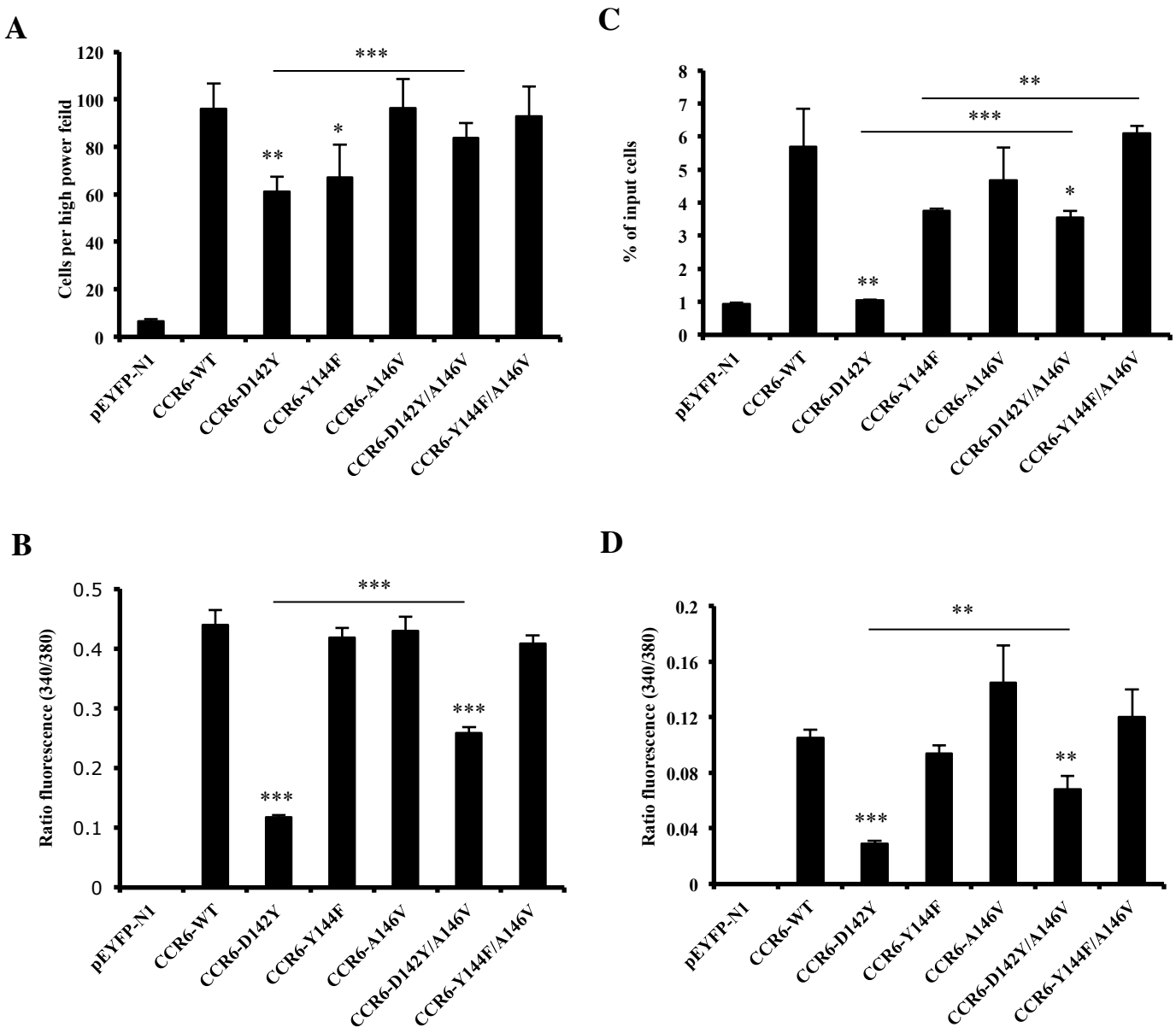

Figure 8